Design and Experiment of a Compact Cable-Driving Module for Reconfigurable Cable-Driven Parallel Robots

Han Yuan
Harbin Institute of Technology
Hao An
Harbin Institute of Technology Shenzhen
Yongqing Zhang
Harbin Institute of Technology Shenzhen
Wenfu Xu (wfxu@hit.edu.cn)
https://orcid.org/0000-0001-8218-6061

Original Article

Keywords: modular design, cable-driving module, reconfigurable robots, cable-driven parallel robots

Posted Date: April 4th, 2020

DOI: https://doi.org/10.21203/rs.3.rs-20465/v1

Title page

Design and Experiment of a Compact Cable-Driving Module for Reconfigurable Cable-Driven Parallel Robots

Han Yuan born in 1987, is currently an assistant professor with *the School of Mechanical Engineering and Automation*, *Harbin Institute of Technology*, *Shenzhen, China.* He received the Ph.D. degree in Mechanical Engineering from Institute National des Sciences Appliquées de Rennes, Rennes, France in 2015. He was a Research Scientist in CNRS UMR6602, Clermont-Ferrand, France from 2015 to 2016 and a Postdoctoral Fellow in the Chinese University of Hong Kong, Hong Kong, China from 2016 to 2017. His research interests include robots, cable-driven manipulator and flexible actuators.
E-mail: yuanhan@hit.edu.cn

Hao An, born in 1994, is currently a PhD candidate at *the School of Mechanical Engineering and Automation, Harbin Institute of Technology, Shenzhen, China*. He received his master degree from *Wuhan University, China,* in 2018. He received his bachelor degree from *Northwest A&F University, China*, in 2014. His research interests include the cable-driven parallel robot, robot control, and robot calibration.
E-mail: 19b953015@stu.hit.edu.cn

Yongqing Zhang, born in 1993. He received his master degree from *Harbin Institute of Technology*, *Shenzhen, China,* in 2020. His research interests include cable-driven parallel robots.
E-mail: yongqing.z@foxmail.com

Wenfu Xu, born in 1979, is currently a professor with *the School of Mechanical Engineering and Automation*, *Harbin Institute of Technology*, *Shenzhen, China.* He received the B.E. degree in 2001, and the M.E. degree in 2003, both in *control engineering, from Hefei University of Technology, Hefei, China*, and the Ph.D. degrees in the c*ontrol science and engineering from Harbin Institute of Technology, Harbin, China*, in 2007. His research interests include reconfigurable robots, space robots and bionic robots.
E-mail: wfxu@hit.edu.cn

Corresponding author：Wenfu Xu　E-mail：wfxu@hit.edu.cn

ORIGINAL ARTICLE

Design and Experiment of a Compact Cable-Driving Module for Reconfigurable Cable-Driven Parallel Robots

Han Yuan[1] • Hao An[1] • Yongqing Zhang[1] • Wenfu Xu[1,2]

Received June xx, 201x; revised February xx, 201x; accepted March xx, 201x

Abstract: Cable-driven parallel robots (CDPRs) have the characteristics of reconfigurability, which endows CDPRs with flexible workspace, freely configurable degrees of freedom and various configurations, greatly expanding their range of applications. Modular design provides great convenience and feasibility for the realization of reconfiguration, which is a key issue of reconfiguration research. However, most existing CDPRs have problems of low modularity and low system integration, which brings inconvenience to the realization of reconfiguration. In this paper, a highly integrated and high precision cable-driving module is designed, which can accurately control the length and tension of the cable. In addition, experimental verification is performed. The single-module experiment shows that the module has good ability for cable length and cable tension control. The cable length control error is less than 0.2mm, and the cable tension control error is less than 0.8N. Furthermore, based on the proposed module, a CDPR with 8 cables and 6 degrees of freedom is constructed rapidly. The open-loop tracking error of the robot is measured by laser tracker. Results show that the tracking error is less than 4.5mm and the Root-Mean-Square-Error (RMSE) is 2.1mm. Besides, the compliance control experiment of the robot shows that the tracking error in impedance control mode is less than 2mm, and the RMSE is 0.95mm, and the drag force in teaching mode is less than 2.5N, which demonstrates good follow-up performance. The proposed compact cable-driving module with high precision could be useful for the design and rapid construction of reconfigurable CDPRs.

Keywords: modular design • cable-driving module • reconfigurable robots • cable-driven parallel robots

✉ Wenfu Xu
wfxu@hit.edu.cn

[1] Harbin Institute of Technology (Shenzhen), Shenzhen 518055, China

[2] State Key Laboratory of Robotics and System, Harbin Institute of Technology, Harbin 150080, China

1 Introduction

In recent years, cable-driven parallel robots (CDPRs) have attracted lots of attentions. They have been widely used in huge telescope [1], rehabilitation [2], live sporting broadcasting [3], disaster rescue [4], virtual reality [5], automatic handling [6], pick-and-place [7-8] large 3D printing [9] and etc. Compared with traditional parallel robots, CDPRs use flexible cables to drive platforms, which makes them have the characteristics of small inertia, large workspace, fast speed and acceleration, strong load capacity, good flexibility and low cost [10-16]. In addition, CDPRs have the characteristics of rapid reconfiguration, which is convenient for disassembly and handling. Various configurations can be obtained according to the specific requirements [17-19].

Modular design is a key to realize reconfiguration of CDPRs, especially the rapid reconfiguration. However, at present, most CDPRs do not consider modular design, and their driving and transmission devices are often installed on the robot frame, so it is difficult to carry out rapid reconfiguration according to the actual requirements. Nevertheless, modular design was onsidered in some previous studies: Seriani proposed a design scheme of modular CDPRs for interplanetary exploration [20]. They divided the main body of the robot into two parts: the module and the end actuator. The module adopts the modular design, including the cable-driving module and the fixed base. This kind of module design is suitable for the scene without fixed base. Gagliardini L et al. Proposed a kind of CDPR, which converted the fixed point of cable connection into the form of moving guide rail [21]. It can change the position of rope connection point according to different environmental requirements to realize the

geometric structure reconstruction, but this form cannot be separated from the dependence on its own guide rail base. J-p. Merlet et al. put forward a modular CDPR lifting equipment which can be used in disaster relief and rescue [22]. The scheme integrates the motor and winch into one module, but the module does not integrate the equipment that can measure the length and tension of the cable accurately. In addition, Gagliardinil et al. put forward the optimization strategy of CDPRs based on graph theory and the reconfiguration strategy based on Dijkstra shortest path algorithm [23-24].

Analysis of the existing researches shows that the key issue to the modular design of CDPRs is the modularization of the cable-driving and controlling device. Functions of most existing modules are still relatively simple, which are not enough in the precise control of cable length and cable tension, and lack cable state acquisition, cable braking and other functions, and thus affect the performances of CDPRs, such as accuracy, safety, reliability and flexibility.

Aiming at the rapid reconfigurable requirements of CDPRs, this paper designs a highly integrated cable driving module which achieves complete functions of drive, transmission, sensing and control. The module integrates an anti-overlapping cable winding bobbin, a servo motor with reducer, an external encoder, a tension sensor and an electromagnetic brake. It has the functions of real-time monitoring of cable length tension, compensation of cable elastic deformation, emergency safety braking, etc. It can not only achieve high-precision cable length control, but also high-precision cable tension control, with good safety and reliability. Besides, we fabricate the prototype of the driving module, and carry out experimental verification, and test the cable length control accuracy and force response performance of the single-mode group. Based on this, we use 8 cable-driving modules to construct a CDPR with 8 cables and 6 degrees of freedom rapidly. In addition, the trajectory tracking accuracy in the open-loop position control mode, the track tracking accuracy in the impedance control mode and the teaching performance in the zero gravity mode are analyzed experimentally. Results show that the module proposed in this paper has good cable length and cable tension control accuracy, and the reconstructed CDPR has good track accuracy.

The rest of this paper is organized as follows: the structural design of the cable driving module is introduced in Section 2; experiments are carried out on a single module in Section 3, including the cable length and cable tension control experiments; section 4 presents an 8-cable and 6-DOF CDPR constructed with the proposed modules. The kinematics accuracy experiments and compliance control experiments are carried out to investigate the trajectory tracking accuracy and force control performance of the CDPR; section 5 is the conclusion of this paper.

2 Structural design of the cable-driving module

This section mainly introduces the proposed cable-driving module, including the overall structure of the module, winding mode, transmission mode, sensor arrangement and routing mode. The cable-driving module is the key part of CDPRs. In order to maximize the reconfigurable performance of CDPRs, the modular design of the cable-driving module is necessary.

2.1 Main structure

The model diagram of the cable-driving module designed in this paper is shown in Figure 1. This module integrates the winding bobbin, servo motor, force sensor, external encoder, electromagnetic brake, as well as the components and transmission devices. In addition to the function of storing cable and controlling cable output, the force sensor is used to detect the cable tension state in real time; the external encoder is used to measure the length of output cable; the limit switch can prevent the winch module from being damaged when the guide rope pulley exceeds the limit position and the electromagnetic brake keeps the tension of the rope to maintain the current state when the robot is powered off. Compared with the previous modular design, this kind of modular design has higher integration and a fuller degree of modularization. Because the drive, transmission, sensing, control and other devices are highly integrated into one module, this module can be used directly to establish CDPRs, and the number and location of module installation can be flexibly selected according to the actual situation. Furthermore, the later maintenance and debugging are more convenient, greatly improving the rapid reconfigurable ability of CDPRs. Meanwhile, through the reasonable design of winding mode, transmission mode, routing mode and sensor layout, this module also has good cable length control accuracy and cable tension control ability. The relevant experimental results are analyzed in the single module experiment in Section 3.

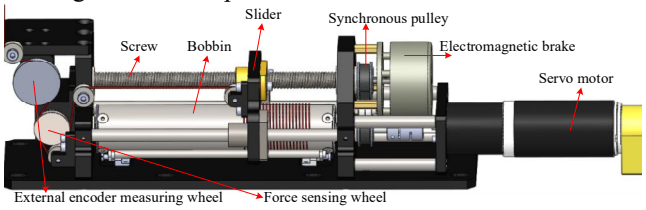

Figure 1 Overall structural of the cable-driving module

2.2 Cable winding device

The cable control accuracy in cable-driving module is mainly determined by the mapping relationship between the winding bobbin and the motor angle. The reasonable cable winding method can guarantee the cable control accuracy of the cable-driving module to a greater extent. For the winding method of CDPRs, the common one is a traditional winch winding. In addition, there are winding bobbins with spiral groove. And this paper proposes the smooth bobbin winding method. The structures of the three winding modes are shown in Figure 2.

a) traditional winch b) bobbin with spiral groove c) smooth bobbin without groove

Figure 2 Three different methods for cable winding

For the traditional winch winding mode, there is no special design for the winding winch, and the cable is directly led out and recovered from the winch. Therefore, this method is easy to stack and stagger cables, which makes cables extremely irregular and difficult to ensure the control accuracy.

To solve the problem that the traditional winch winding is difficult to control the cable accuracy, some scholars put forward a bobbin winding method with spiral groove [25]. This method avoids the situation that cable is stacked and staggered with each other in winch winding method, and spiral groove matching with cable is added on the bobbin, so as to better avoid the sliding of the cable on the bobbin. However, because of friction, wriggle of the cable is more obvious. In addition, because of the difficulty in spiral groove machining, it is easy to have inconsistent depth during the processing. And there are also problems in matching the cable with the initial position of the spiral groove; besides, this spiral groove can only be suitable for cables with a specific diameter range, while others are not easy to maintain high-precision control, so the general performance of this bobbin is not good.

In order to solve problems in spiral groove bobbin winding method, a smooth bobbin winding method is adopted in this paper. Compared with the spiral groove, the machining accuracy of the smooth bobbin can be better guaranteed, and it can be suitable for cables with different diameters and materials. By means of guide pulley and screw, the cable can be evenly wound on the drum in a spiral form, which greatly relieves wriggle of the cable, so the control accuracy of the cable length is more accurate. In addition, the smooth bobbin does not have problems in matching the spiral groove with the cable, which is more convenient for installation, debugging and cable replacement.

2.3 Transmission module

The transmission part of the cable-driving module includes servo motor, coupling, synchronous pulley driving mechanism, screw driving mechanism, circular guide rail and winding bobbin. From the model diagram in Figure 1, the output end of servo motor and the input end of winding bobbin are connected by coupling; the coupling adopts elastic quincunx coupling, which can effectively reduce vibration and compensate radial, angular and shaft errors. The screw and the circular guide rail are used to fix the guide pulley, through which the spiral winding can be carried out on the winding bobbin. The circular guide rail is arranged symmetrically, which is easy to install and highly reliable. The winding bobbin is arranged below the transmission screw, which reduces the volume of the module, makes the screw more uniform and improves the service life of screw.

2.4 Sensor arrangement and cable layout

Through the reasonable arrangement of cable layout, the acquisition accuracy of the sensor can be greatly improved. The sensor arrangement and cable layout are shown in Figure 3. One end of the cable is fixed on the cable bobbin. After passing through the bobbin, the cable first passes through the guide pulley, and then passes through the force sensing wheel at the measuring end of the force sensor. The force sensor is used for measuring the cable tension, and the cable is pressed on the force sensing wheel from the left side to the top with 120 degrees. After coming out from the force sensing wheel, the cable passes through the external encoder measuring wheel used for measuring the output length of the cable. The external encoder measuring wheel is connected with the input end of the external encoder through a flexible coupling. The force sensor is arranged in front of the external encoder to avoid the effect of the vibration of the cable on the force information collection. The external encoder arranged at the outermost end of the module can measure the actual output length of the cable more directly. In order to improve the accuracy of cable control, this paper adopts the control method of external encoder measurement combined with cable elastic deformation compensation. The output length of the cable is measured by the external encoder, and the cable deformation at the end platform and the output end of the

module is superimposed to obtain the actual cable length. The calculation formula can be written as:

$$L_r = \frac{D_e\theta_e}{2} + \frac{FL_c}{EA} \quad (1)$$

Where:

D_e is the diameter of the measuring wheel of the external encoder;

θ_e is the angle of the measuring wheel of the external encoder;

F is the tension of the cable;

E is the Young's modulus of the cable;

A is the cross-sectional area of the cable;

L_c is the theoretical length of the cable;

L_r is the actual length of the cable;

The Young's modulus of the cable can be obtained through the Young's modulus calibration experiment.

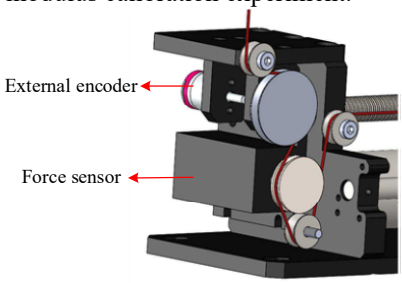

Figure 3 Sensor arrangement and cable layout

3 Single cable-driving module experiment

The control accuracy of cable length and cable tension are two important indexes for cable-driving module. In the process of modular design, the cable-driving module should not only improve the rapid reconfigurable performance of CDPRs, but also have good cable length and cable tension control accuracy. Therefore, we carried out the cable length control accuracy experiment and cable tension response performance experiment for a single module, and the experimental setup is shown in Figure 4.

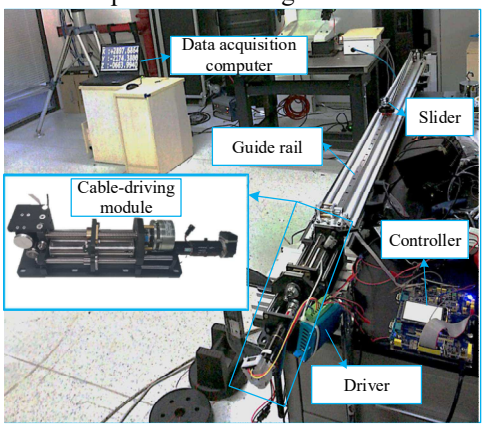

Figure 4 Experimental setup for the single cable module tests

In the experiment, the module is fixed on one end of the guide rail and the cable is led out from the module fixed by the slider, then it is connected with the load at the other end of the guide rail after passing through the slider. The target ball of the laser tracker is placed on the slider to measure the actual length of the cable. We choose API series laser tracker, whose three-dimensional spatial position measurement accuracy is 0.015mm; The external encoder adopts 12 unit aperture absolute encoder, and the angle measurement accuracy is 0.0879 degrees and Maxon RE35 DC brush motor is selected, with rated output torque of 106 Nm and maximum speed of 5760rpm. The reducer is Maxon GP22C, the reduction ratio is 16, and the transmission efficiency is 0.95. The lead of screw is 2mm and the diameter of drum is 30mm.

3.1 Cable length control

During the operation of the cable-driving module, the end of the cable will be subject to the constantly changing tension. Therefore, in order to analyze the cable length control accuracy of the driving module under the condition of changing load, we install a tension spring at the output end of the module to keep the initial value of the rope force at 30N. The motor releases the cable 180 degrees each time (corresponding to the cable length change of 47.12mm), so that the cable tension decreases gradually. We took the actual length of the cable measured by the laser tracker as a reference, and compared with the results measured by the embedded encoder of the motor, the measurement results of the external encoder of the module, and the cable length calculated by means of external encoder measurement combined with cable elastic deformation compensation. Meanwhile, the accumulated errors in the process of the motor angle change are calculated respectively. The results are shown in Figure 5.

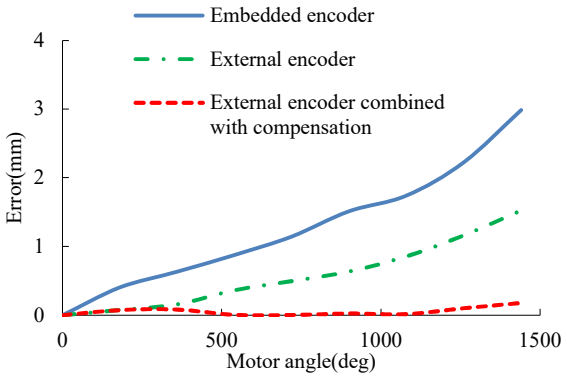

Figure 5 Comparison of the accumulated errors of the cable length measured by embedded motor encoder, external encoder and external encoder with compensation

From the accumulated error results of the embedded encoder and external encoder, it is clear that the

accumulated error of the cable length measurement increases gradually with the increase of the motor angle. When the motor angle increases to 1440 degrees, the accumulated error of embedded encoder is 2.98mm. The external encoder can reduce it to 1.52mm. In addition, when external encoder measurement combined with cable elastic deformation compensation is used, the accumulated error is small and the maximum error is 0.178mm. Consequently, compared with the general method of cable length measurement, the cable-driving module designed in this paper has smaller accumulated error of cable length measurement in the process of cable tension change and better cable length control accuracy.

3.2 Cable tension control

In order to realize the impedance control [26-27], the cable-driving module of CDPRs needs to have a good precision of the force control. According to the actual situation of force control, we plan step force response experiment, ramp force response experiment and dynamic force response experiment respectively to analyze the accuracy of cable tension control of cable-driving module.

In the step force response experiment, a step force signal from 10N to 15N is given to the module. Figure 6 shows the actual force response curve, the desired force response curve and the error between the actual force and the desired force under the action of step force signal.

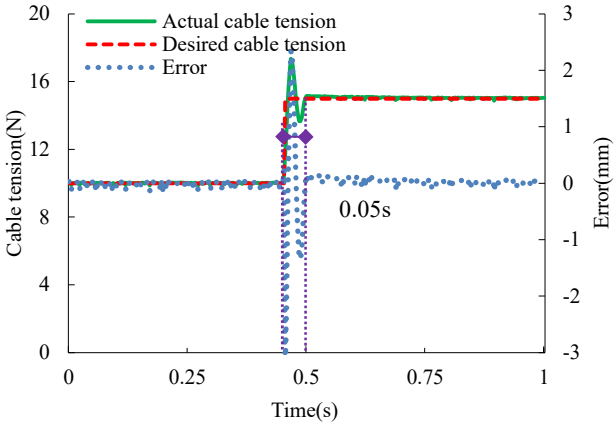

Figure 6 Response of the module with step signal input: actual cable tension, desired cable tension and their error

Before the step response, the actual cable tension and the desired cable tension are both 10N. When receiving the step force signal, the actual cable tension responds rapidly. After 0.05 seconds of oscillation, it is stable to the desired cable tension. Its RMSE is 0.07N, which has good step force response performance.

In the ramp force response experiment, the rope maintains 8N tension at first, and then sends the slope force control signal from 10N to 30N to module within 5 seconds. Figure 7 illustrates the actual force response curve, the desired force response curve and the error change between the actual force and the desired force.

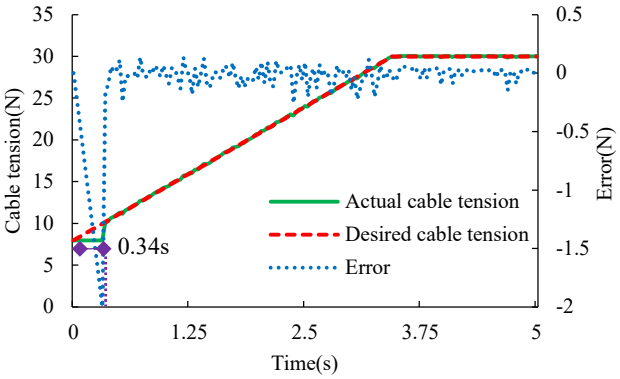

Figure 7 Response of the module with ramp signal input: actual cable tension, desired cable tension and their error

Under the signal of ramp force, cable tension reaches to 10N rapidly in 0.34 seconds and increases accurately with the desired cable tension curve and is stable at 30N. The RMSE of the actual cable tension in ramp process is 0.22N and the RMSE of the stable cable tension is 0.04N. As a result, the module proposed in this paper has good ramp force response performance.

Dynamic force response experiment is to verify the force retention performance of the cable in the process of motion. The cable tension is kept at 10N at first, then the module drives the cable to move back and forth and records the actual cable tension data in real time. Figure 8 displays the results of dynamic force response experiment.

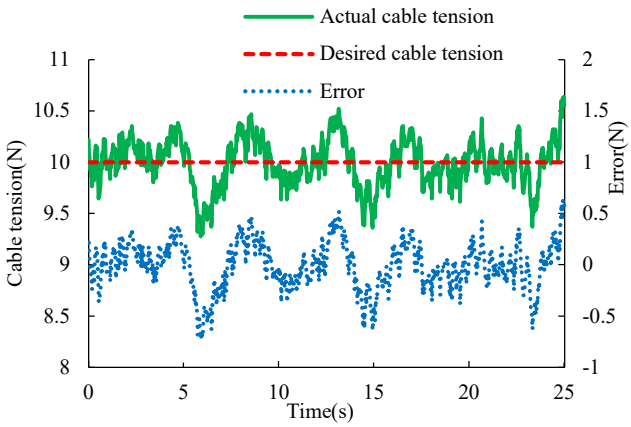

Figure 8 Variation of the actual cable tensions in reciprocating movement: actual cable tension, desired cable tension and their error

According to the experiment results, there are only small floating variations for cable tension in the back and forth process. After calculation, the RMSE of the cable tension is 0.23N, and the maximum error is 0.72N. This means that the cable-driving module in this paper has pretty good ability in force retention performance.

Summarily, the cable-driving module designed in this paper has good control accuracy of cable tension and good dynamic response.

4 Experiments on a 6-DOF CDPR driven by 8 modules

In addition to the good performance of the signal module, CDPRs constructed with modules designed in this paper also needs to have good performance. As a result, a CDPR with 8 cables and 6 degrees of freedom is built rapidly. Figure 9 shows the model of this CDPR; Table 1 displays its configuration parameters, including attachment points $B_i(i = 1{\sim}8)$ expressed in global frame and attachment points $A_i(i = 1{\sim}8)$ expressed in local frame. Additionally, the kinematic accuracy experiment and compliance control experiment of the CDPR are carried out. Figure 10 shows the layout of experiment site. The actual trajectory of the end moving platform is measured by the API laser tracker and compared with the desired trajectory of the robot.

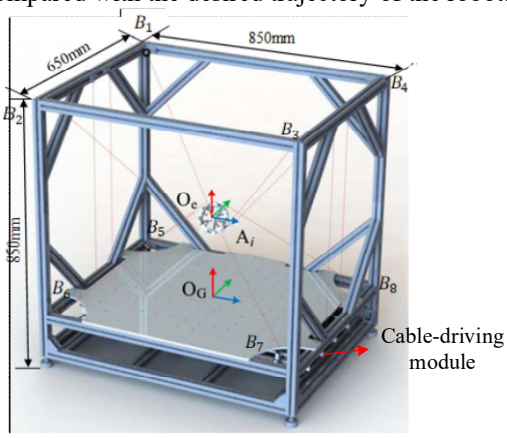

Figure 9 Structure of the 6-DOF CDPR driven by 8 cables

Table 1 Geometric parameters of the CDPR (A_i expressed in local frame O_e; B_i expressed in global frame O_G)

Attachment point	X（mm）	Y（mm）	Z（mm）
A1	-42.6	30.9	-26.3
A2	-42.6	-30.9	-26.3
A3	16.2	-50.1	-26.3
A4	16.2	50.1	-26.3
A5	-16.2	50.1	26.3
A6	-16.2	-50.1	26.3
A7	42.6	-30.9	26.3
A8	42.6	30.9	26.3
B1	-406.6	291.5	672.8
B2	-396.3	-306.7	671.7
B3	397.5	-297.3	671.7
B4	387.3	301.5	671.5
B5	-404.0	291.6	3.4
B6	-396.7	-305.0	4.3
B7	398.9	-296.6	5.9
B8	391.7	300.8	5.8

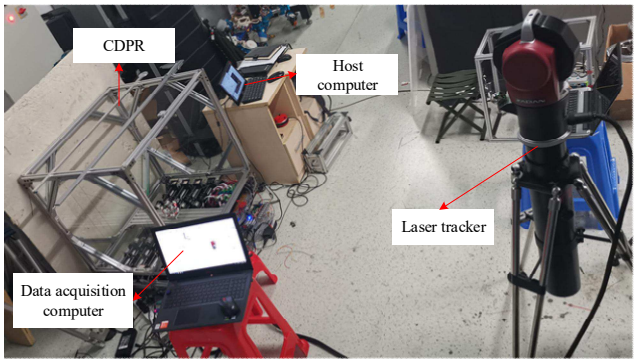

Figure 10 Experimental setup for the 6-DOF CDPR tests

4.1 Kinematic accuracy experiments

First, the desired trajectory of the CDPR moving platform is given, then the desired length of eight cables is calculated through the inverse kinematics of the CDPR [28], and eight cable-driving modules are operated in the cable length control mode. The actual position of the CDPR moving platform is measured by the laser tracker and the error between the actual trajectory and the desired trajectory can be calculated. Consequently, the open-loop accuracy of the CDPR in the position control mode can be evaluated. In this section, experiments of plane line trajectory, plane circle trajectory and space spiral trajectory are carried out. These three experiments are without load. Moreover, experiment of circle trajectory under large load is analyzed too.

In the plane line trajectory experiment, the line trajectory running in the XOY plane is selected for analysis when Z coordinate is 200 mm. Figure 11 shows the actual trajectory, the desired trajectory and the distance error between them based on the X axis.

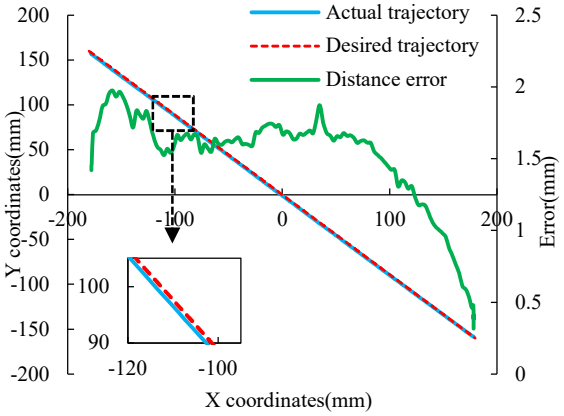

Figure 11 Line trajectory test: actual trajectory, desired trajectory and their error

Comparing the actual trajectory with the desired trajectory, it is observable that the actual trajectory is closed to the desired trajectory. The maximum error of distance

error is 1.97mm, the RMSE is 1.54mm. This confirm that the actual line trajectory has a good accuracy.

In the plane circle trajectory experiment, the circle running in the XOY plane is selected for analysis when Z coordinate is 200 mm. The radius of the circle is 150 mm. The trajectory starts from point (150,0) and rotates one circle in the counterclockwise direction. Figure 12 displays the actual circle trajectory, the desired circle trajectory, and the distance error between them.

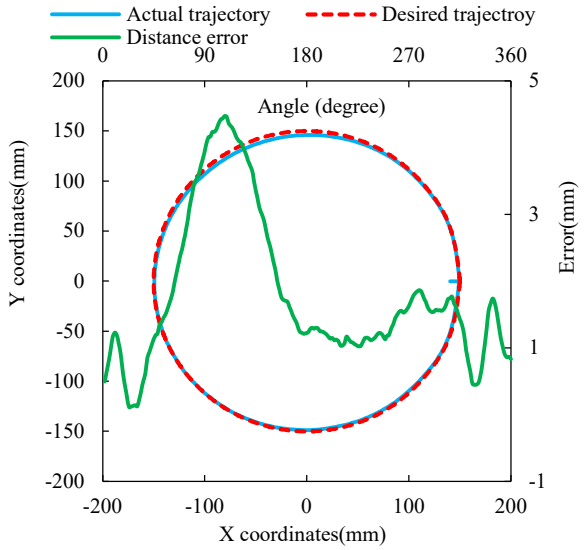

Figure 12 Circle trajectory test: actual trajectory, desired trajectory and their error

According to the results in Figure 12, the maximum distance error between the actual trajectory and the desired trajectory is 4.47mm, and the RMSE is 2.11mm, which indicates that there is a good precision when running the circle trajectory.

The spiral trajectory selected in this paper has a rising pitch of 100 mm and a spiral radius of 150 mm. Figure 13 shows the desired spiral trajectory and the actual spiral trajectory. Meanwhile, Figure 14 illustrates the distance errors between the actual spiral trajectory and the desired spiral trajectory. The maximum distance error between the actual spiral trajectory and the desired spiral trajectory is 3.73mm, the RMSE is 2.09mm. As a result, the space spiral trajectory has good control accuracy.

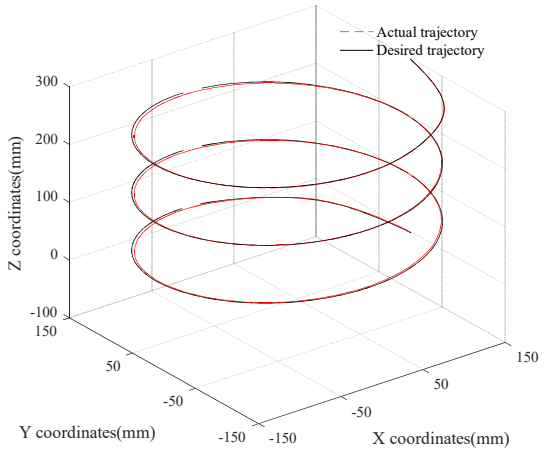

Figure 13 Space spiral trajectory test: actual trajectory and desired trajectory

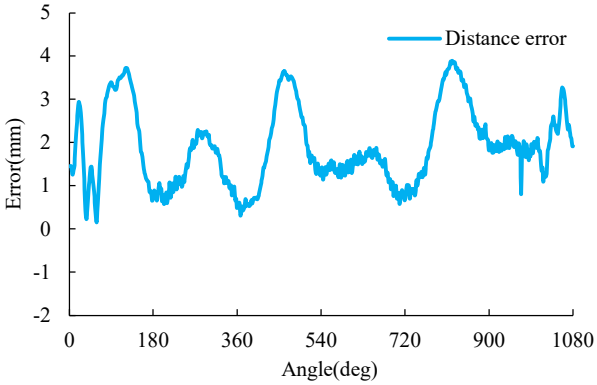

Figure 14 Error of the spiral trajectory test.

In addition to different trajectories, it is important for CDPRs to have good trajectory accuracy under large load, so we carried out trajectory accuracy experiment under large load. 2kg load is added at the moving platform and a circle trajectory the same as before is selected in XOY plane when Z coordinate is 200mm. The laser tracker is used to record the actual position of the moving platform in real time. By comparing the positions of desired trajectory and actual trajectory, Figure 15 shows the distance errors between desired trajectory and actual trajectory under large load.

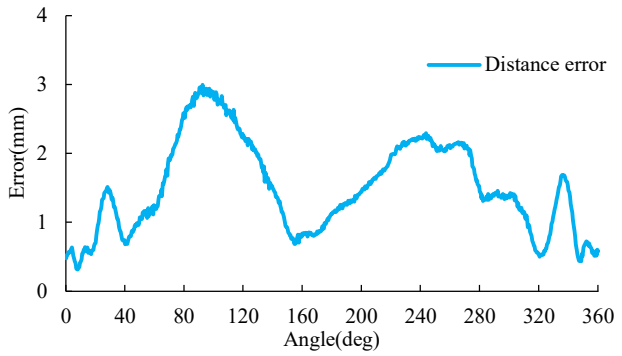

Figure 15 Errors of the circle trajectory between desired trajectory and actual trajectory under large load condition

From calculation results in Figure 15, the maximum distance error between the actual trajectory and the desired trajectory is 2.99mm, and the RMSE is 1.65mm. Obviously, the CDPR proposed in this paper has good trajectory control accuracy under the condition of large load.

In general, through the trajectory accuracy experiments under no load and large load conditions, the maximum error of the open-loop trajectory accuracy of the CDPR constructed by modules mentioned in this paper is no more than 4.5mm when it is running under different conditions. Compared with the overall size of the robot 850X650X650 mm^3, it has a good open-loop trajectory accuracy.

4.2 Compliance control experiment

Section 4.1 verify the kinematic accuracy of the modular CDPR and the precise cable length control ability of the cable-driving module. In this section, to verify the force control ability of the module, the compliance control experiments are carried out, including the track following experiment in impedance mode and the direct teaching experiment in zero-gravity mode.

4.2.1 Trajectory tracking experiment in impedance control mode

The force-based impedance control method of the CDPR in this paper consists of two main control loops, one is the large loop of impedance control and the other is the small loop of cable tension control [29-31]. Figure 16 shows the control block diagram.

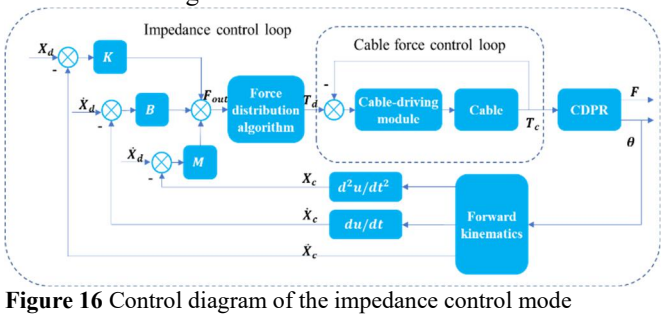

Figure 16 Control diagram of the impedance control mode

In the whole control process, the current module angle obtains the moving platform pose state through the robot forward kinematics at first [32]. After that, the moving platform force is obtained by the force-based impedance control model. The force-based impedance control model is expressed as:

$$F_{out} = K(X_d - X_c) + B(\dot{X}_d - \dot{X}_c) + M(\ddot{X}_d - \ddot{X}_c) \quad (2)$$

Where:

F_{out} is the moving platform;

K is the stiffness matrix;

B is the damping matrix;

M is the inertia matrix;

X_d is the desired end position;

X_c is the actual end position.

The desired force T_d of each cable can be solved by F_{out} through the force distribution algorithm. Then, according to the difference between the desired cable tension T_d and the actual cable tension T_c, the actual cable tension can be adjusted through the small loop of cable tension control, so as to complete the impedance control.

The force distribution algorithm in this paper adopts the following methods: according to the virtual work principle [33], the relationship between the cable tension and the external force of the moving platform is as follows:

$$\boldsymbol{J}^T\boldsymbol{F} + \boldsymbol{W_{ex}} = 0 \quad (3)$$

Where:

$\boldsymbol{J}$ is the Jacobian matrix of moving platform pose and cable length;

$\boldsymbol{F} = [F_1, F_2 \ldots F_8]^T$ is the force of 8 cables;

$\boldsymbol{W_{ex}}$ is the external force and external moment.

From formula (3), $\boldsymbol{J}^T$ is a matrix of 6 rows and 8 columns, the number of equations is 6, the number of unknowns is 8, so the distribution of $\boldsymbol{F}$ has infinite solutions and constraints need to be added to optimize the solution. As a result, the optimization objective function is established based on the principle of minimum energy consumption in this paper. Its constraint equation formula is as follows:

$$F_{min} = \sum_{i=1}^{8} {F_i}^2 \ (i = 1\sim8) \quad (4)$$

In addition, since the cable can only produce pull force, which means the value of cable tension must be positive, so the value of cable tension has a lower limit of F_{min}; Moreover, because of the limitation of motor power, the force of cable can not be increased infinitely, there are also an upper limit of F_{max}, which can be expressed by the formula:

$$F_{min} \le F_i \le F_{max} \ (i = 1\sim8) \quad (5)$$

The trajectory tracking experiment in impedance control mainly verifies the trajectory tracking accuracy and the cable tension following accuracy of CDPR after the

application of impedance control. The same line trajectory as Section 4.1 is selected as research object, and the distance error between the actual and desired trajectory is analyzed, which is shown in Figure 17.

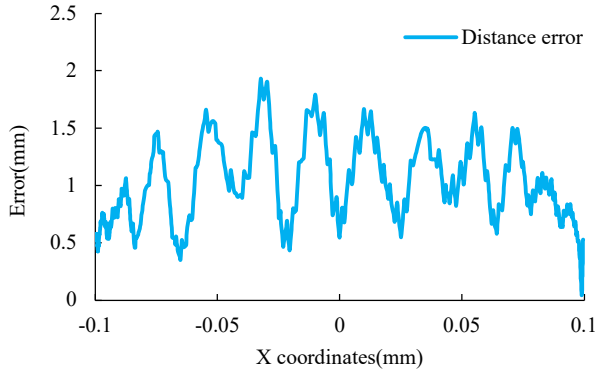

Figure 17 Trajectory tracking error between the actual and desired end-effector positions under impedance control mode

According to the result of Figure 17, the maximum distance error is 1.93mm, and the RMSE is 0.97mm. Therefore, the robot's trajectory has good accuracy under the impedance tracking.

For the following accuracy of the cable tension, this paper selects the No. 4 cable-driving module as the research object, and analyzes the following accuracy by comparing the errors between the actual cable tension and the desired cable tension. Figure 18 shows the desired cable tension curve, the actual cable tension curve and errors between them. It is clear that the cable tension has a good following accuracy, with the maximum error of 1.06N and the RMSE of 0.31N after calculation.

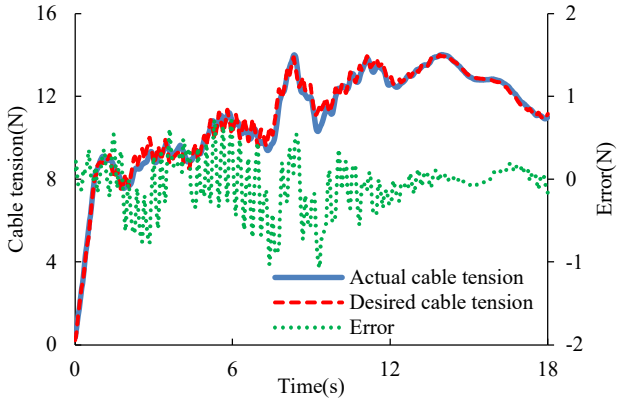

Figure 18 Variation of the cable tension in one of the 8 modules: desired cable tension, the actual cable tension and their error

4.2.2Direct teaching experiment in zero-gravity mode

In this paper, the zero-gravity control method based on joint torque is used to realize the direct teaching [34]. A six-dimensional force sensor is installed at the moving platform of the CDPR to collect the drag force between the hand and the moving platform in real time. The total mass of the sensor and the connecting piece is 379.8g, so the program approximately uses 3.8N to compensate the gravity. In order to test the flexibility of the moving platform, the approximate triangle trajectory is dragged randomly during the experiment, and the actual drag force of the moving platform are recorded in real time. Figure 19 displays the drag force curve of the moving platform in three directions. Among them, the maximum drag force in X direction is 2.38N, the maximum drag force in Y direction is 0.95N, and the maximum drag force in Z direction is 1.93N. Obviously, the drag force is relatively small in all directions, thus, the CDPR has good drag flexibility in zero-gravity mode.

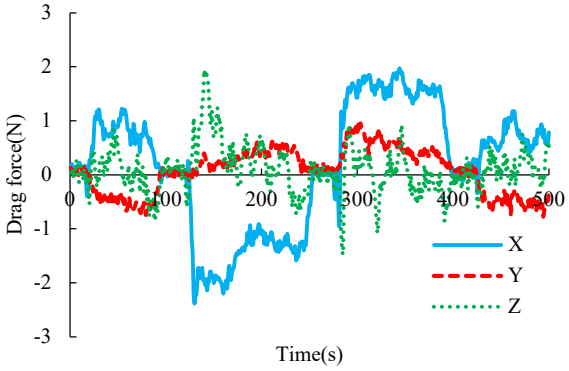

Figure 19 Variation of the drag force on the moving platform in three directions under direct teaching test

5 Conclusions

This paper designs a highly integrated cable driving module, which has good accuracy in cable length and cable tension controlling. The experimental results show that the cable length control error is less than 0.2mm, the cable tension control error is less than 0.8N, and the response time of the module is less than 0.05s for a step signal input, which has good dynamic response.

In addition, a CDPR with 8 cables and 6 DOFs is constructed of the proposed module. Experiments of kinematic accuracy and compliance control are carried out respectively. The open-loop trajectory tracking errors are all less than 4.5mm under both position and impendence control modes. Results show that the module proposed in this paper can reconstruct a CDPR quickly while achieving good accuracy.

The module in this paper integrates driving, transmission, sensing, and control functions. It realizes the high integration of the module. Rapid construction and reconstruction of modular CDPRs can be completed by the modules. In the future, the performance of the CDPR can be further improved by combining with more advanced control algorithms.

6 Declaration

Acknowledgements
Not applicable

Funding
Supported by National Natural Science Foundation of China (Grant No. 61803125), Basic Research Program of Shenzhen (Grant No. JCYJ20190806144416980), National Key R&D Program of China (2018YFB1304600), Key Research and Development Program of Guangdong Province (2019B090915001).

Availability of data and materials
The datasets supporting the conclusions of this article are included within the article.

Authors' contributions
The author' contributions are as follows: Wenfu Xu and Han Yuan were in charge of the whole trial; Han Yuan and Hao An wrote the manuscript; Yongqing Zhang and Hao An supported mechanical design and assisted with sampling and laboratory analyses.

Competing interests
The authors declare no competing financial interests.

Consent for publication
Not applicable

Ethics approval and consent to participate
Not applicable

References

[1] Nan R, Li D, Jin C, et al. The Five-Hundred-Meter Aperture Spherical Radio Telescope (FAST) Project. *International Journal of Modern Physics D*, 2011, 20(06) :989-1024

[2] Mao Y, Agrawal S K. Design of a Cable-Driven Arm Exoskeleton (CAREX) for Neural Rehabilitation. *IEEE Transactions on Robotics*, 2012, 28(4) : 922-931.

[3] Tanaka M, Seguchi Y, Shimada S. Kineto-Statics of Skycam-Type Wire Transport System. *Proceedings of USA-Japan symposium on flexible automation, Crossing bridges: advances in flexible automation and robotics*. 1988 : 689-694.

[4] S. Tadokoro, R. Verhoeven, M. Hiller, T. Takamori, A portable parallel manipulator for search and rescue at large-scale urban earthquakes and an identification algorithm for the installation in unstructured environments. *Proceedings of the IEEE/RSJ International Conference on Intelligent Robots and Systems*, IROS'99, vol. 2, 1999, pp. 1222–1227.

[5] Kljuno E, Williams R L. Vehicle Simulation System: Controls and Virtual-Reality Based Dynamics Simulation. *Journal of Intelligent and Robotic Systems*, 2008, 52(1) : 79-99.

[6] Bostelman R, Albus J, Dagalakis N, et al. Applications of the NIST Robo Crane. *Proceedings of the 5th International Symposium on Robotics and Manufacturing*, 1994 : 14-18.

[7] J. Lamaury and M. Gouttefarde, "Control of a Large Redundantly Actuated Cable-Suspended Parallel Robot," presented at the *ICRA'2013: International Conference on Robotics and Automation,* 2013, pp. 4644–4649.

[8] H. Yuan, E. Courteille, M. Gouttefarde, and P.-E. Hervé. Vibration analysis of cable-driven parallel robots based on the dynamic stiffness matrix method. *Journal of Sound and Vibration*, vol. 394, pp. 527–544, Apr. 2017.

[9] Izard J B, Dubor A, Hervé P-E, et al. Large-Scale 3D Printing with Cable-Driven Parallel Robots. *Construction Robotics*, 2017, 1(1-4) : 69-76.

[10] P. Bosscher, R.L. Williams, M. Tummino. A concept for rapidly-deployable cable robot search and rescue systems. *Proceedings of the ASME International Design Engineering Technical Conferences and Computers and Information in Engineering Conference, American Society of Mechanical Engineers*, 2005, pp. 589–598.

[11] Tang X. An Overview of the Development for Cable-Driven Parallel Manipulator. *Advances in Mechanical Engineering*, 2014, 6 : 1-9

[12] J.-P. Merlet, Marionet. a family of modular wire-driven parallel robots. *Advances in Robot Kinematics, Motion in Man and Machine*, Springer, 2010,pp. 53–61

[13] J.-P. Merlet. Parallel robots. Springer, 2006, vol. 128

[14] J. Lamaury and M. Gouttefarde. Control of a large redundantly actuated cable-suspended parallel robot. *Robotics and Automation(ICRA)*, 2013 IEEE International Conference on. IEEE, 2013, pp. 4659–4664.

[15] B. Zi, B. Duan, J. Du, and H. Bao. Dynamic modeling and active control of a cable-suspended parallel robot. *Mechatronics*, vol. 18, no. 1, pp. 1–12, 2008.

[16] Han Yuan, Eric Courteille , Dominique Deblaise. Static and dynamic stiffness analyses of cable-driven parallel robots with non-negligible cable mass and elasticity. *Mechanism and Machine Theory*, Volume 85, March 2015, Pages 64-81

[17] Qian S, Zi B, Shang W, et al. A Review on Cable-Driven Parallel Robots. *Chinese Journal of Mechanical Engineering*, 2018, 31(1) : 66-76.

[18] Y. Mao, S.K. Agrawal. Design of a cable-driven arm exoskeleton (CAREX) for neural rehabilitation. *IEEE Trans. Robot*, 28 (4) (2012) 922–931.

[19] Yuan H, You X, Zhang Y, et al. A Novel Calibration Algorithm for Cable-Driven Parallel Robots with Application to Rehabilitation. *Applied Sciences*, 2019, 9(11) :1-9

[20] Seriani S, Gallina P, Wedler A. A Modular Cable Robot for Inspection and Light Manipulation on Celestial Bodies. *Acta Astronautica*, 2016, 123 : 145-153.

[21] Gagliardini L, Caro S, Gouttefarde M, et al. A Reconfigurable Cable-Driven Parallel Robot for Sandblasting and Painting of Large Structures. *Cable-Driven Parallel Robots*. [S.l.] : Springer, 2015 : 275-291

[22] Merlet J P, Daney D. A portable, modular parallel wire crane for rescue operations. *IEEE International Conference on Robotics and Automation*, ICRA 2010, Anchorage, Alaska, USA, 3-7 May 2010. IEEE, 2010.

[23] Gagliardini L, Caro S, Gouttefarde M, et al. Discrete Reconfiguration Planning for Cable-Driven Parallel Robots.

Mechanism and Machine Theory, 2016, 100 : 313-337.
[24] Carricato M. Direct Geometrico-Static Problem of Underconstrained Cable-Driven Parallel Robots with Three Cables. *Journal of Mechanisms and Robotics*, 2013, 5(3) : 1-9.
[25] Yuan H, Zhang Y, Xu W. Design and Experiments of a Redundantly Actuated Cable-Driven Parallel Robot. *2018 IEEE International Conference on Robotics and Biomimetics (ROBIO)*. 2018 : 928-933.
[26] Reichert C , Katharina Muller, Bruckmann T. Internal Force-Based Impedance Control for Cable-Driven Parallel Robots, Advances on Theory and Practice of Robots and Manipulators. *Proceedings of Romansy 2014 XX CISM-IFToMM Symposium on Theory and Practice of Robots and Manipulators*, Springer International Publishing, 2014.
[27] Hogan N. Impedance Control: An Approach to Manipulation. *1984 American Control Conference*, 1984 : 304-313.
[28] Gao B , Song H , Zhao J , et al. Inverse kinematics and workspace analysis of a cable-driven parallel robot with a spring spine. *Mechanism and Machine Theory*, 2014, 76:56-69.
[29] Ortega R, Loria A, Nicklasson PJ, Sira-Ramirez H. Passivity-based control of EulerLagrange systems, 1st edn. Springer, New York
[30] Caccavale F, Siciliano B, Villani L. The Tricept robot: dynamics and impedance control. *IEEE / ASME Transactions on Mechatronics*, 2003, 8(2):p.263-268.
[31] Bruzzone L, Callegari M. Application of the Rotation Matrix Natural Invariants to Impedance Control of Rotational Parallel Robots, Advances in Mechanical Engineering, 2010, 2(2 Pt 1):79-97.
[32] Schmidt V, Pott A. Implementing Extended Kinematics of a Cable-Driven Parallel Robot in Real-Time. 2013.
[33] H. Yuan, E. Courteille, and D. Deblaise, Force Distribution With Pose-Dependent Force Boundaries for Redundantly Actuated Cable-Driven Parallel Robots. *J. Mechanisms Robotics*, vol. 8, no. 4, Aug. 2016.
[34] Kushida D, Nakamura M, Goto S, et al. Human direct teaching of industrial articulated robot arms based on force-free control. *Artificial Life & Robotics*, 2001, 5(1):26-32.

Biographical notes

Han Yuan born in 1987, is currently an assistant professor with *the School of Mechanical Engineering and Automation*, *Harbin Institute of Technology*, *Shenzhen, China.* He received the Ph.D. degree in Mechanical Engineering from Institute National des Sciences Appliquées de Rennes, Rennes, France in 2015. He was a Research Scientist in CNRS UMR6602, Clermont-Ferrand, France from 2015 to 2016 and a Postdoctoral Fellow in the Chinese University of Hong Kong, Hong Kong, China from 2016 to 2017. His research interests include robots, cable-driven manipulator and flexible actuators.
E-mail: yuanhan@hit.edu.cn

Hao An, born in 1994, is currently a PhD candidate at *the School of Mechanical Engineering and Automation, Harbin Institute of Technology, Shenzhen, China*. He received his master degree from *Wuhan University, China,* in 2018. He received his bachelor degree from *Northwest A&F University, China*, in 2014. His research interests include the cable-driven parallel robot, robot control, and robot calibration.
E-mail: 19b953015@stu.hit.edu.cn

Yongqing Zhang, born in 1993. He received his master degree from *Harbin Institute of Technology*, *Shenzhen, China,* in 2020. His research interests include cable-driven parallel robots.
E-mail: yongqing.z@foxmail.com

Wenfu Xu, born in 1979, is currently a professor with *the School of Mechanical Engineering and Automation*, *Harbin Institute of Technology*, *Shenzhen, China.* He received the B.E. degree in 2001, and the M.E. degree in 2003, both in *control engineering, from Hefei University of Technology, Hefei, China*, and the Ph.D. degrees in the c*ontrol science and engineering from Harbin Institute of Technology, Harbin, China*, in 2007. His research interests include reconfigurable robots, space robots and bionic robots.
E-mail: wfxu@hit.edu.cn

Appendix

Not applicable

Figures

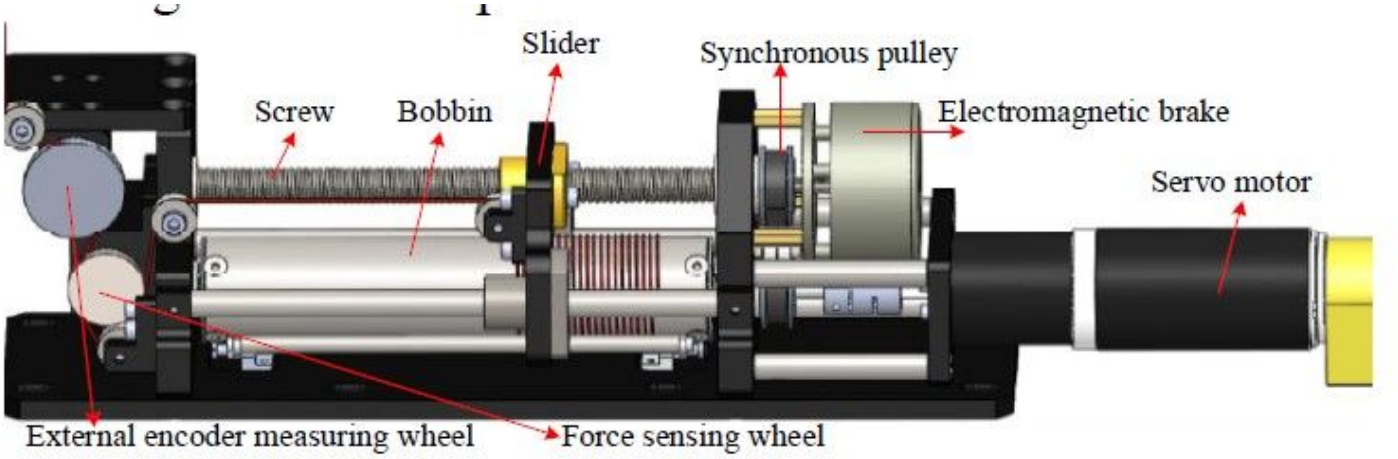

Figure 1

Overall structural of the cable-driving module

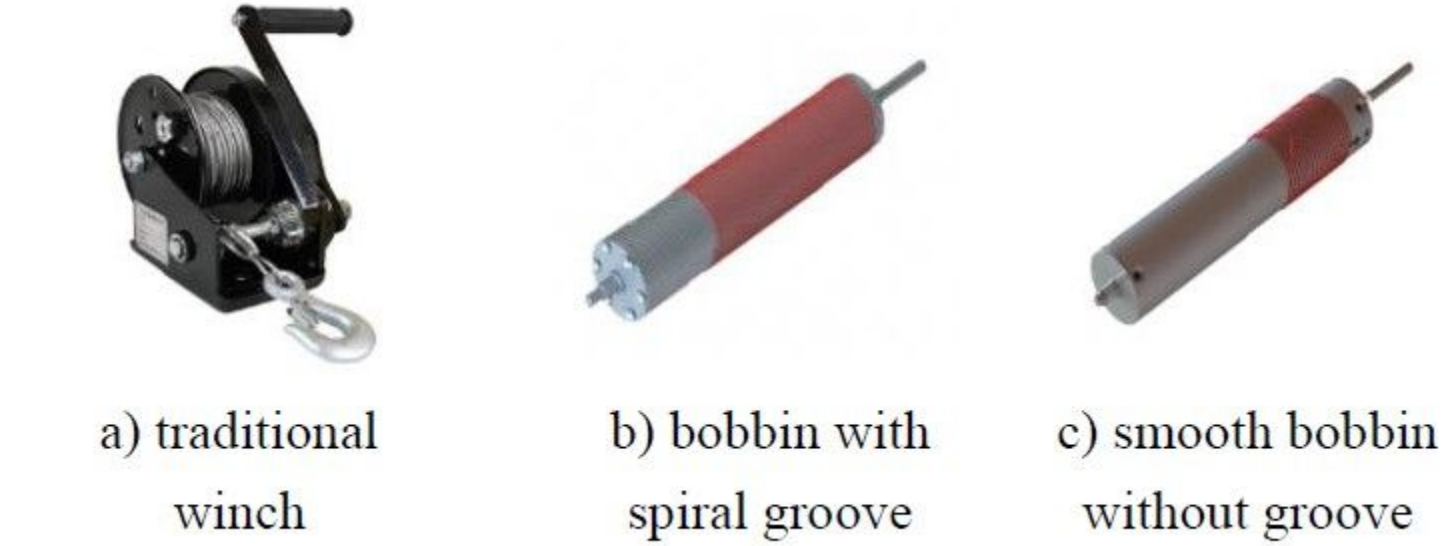

Figure 2

Three different methods for cable winding

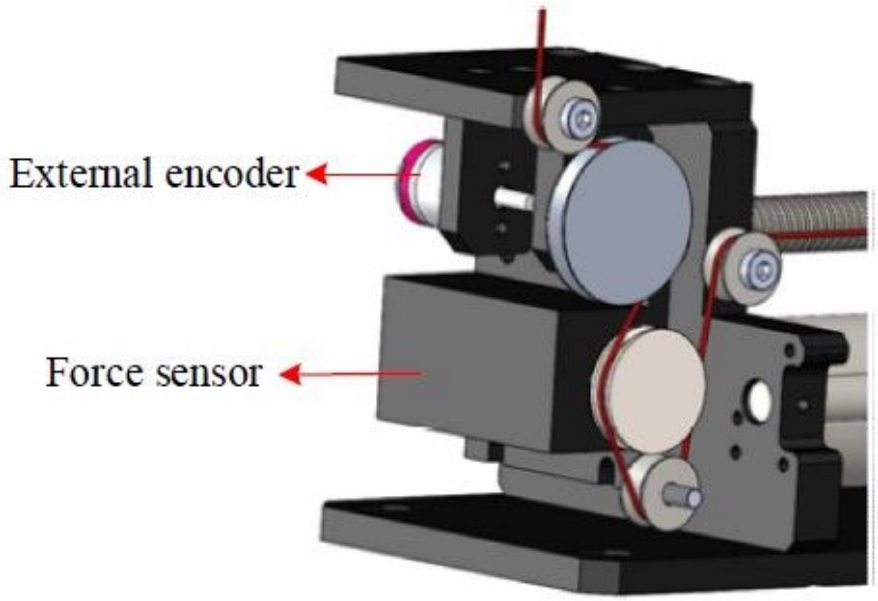

Figure 3

Sensor arrangement and cable layout

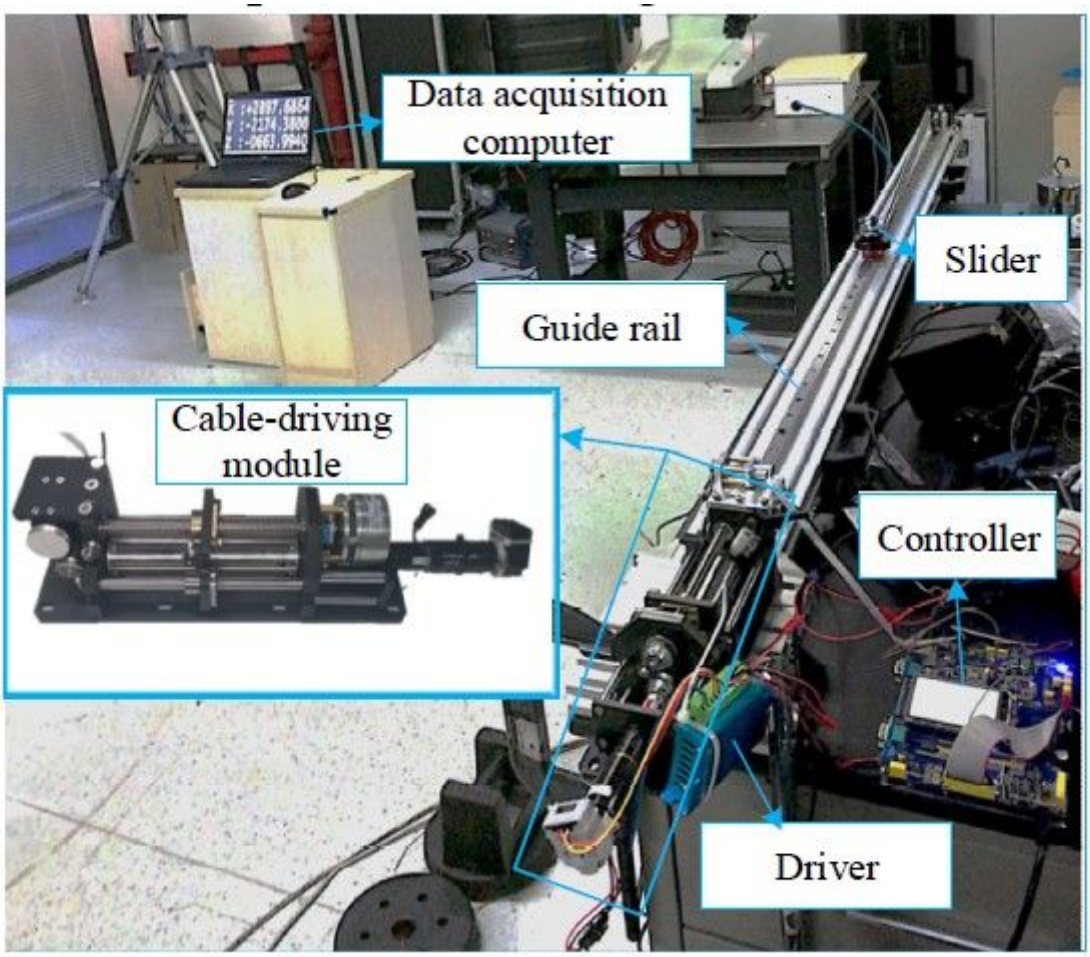

Figure 4

Experimental setup for the single cable module tests

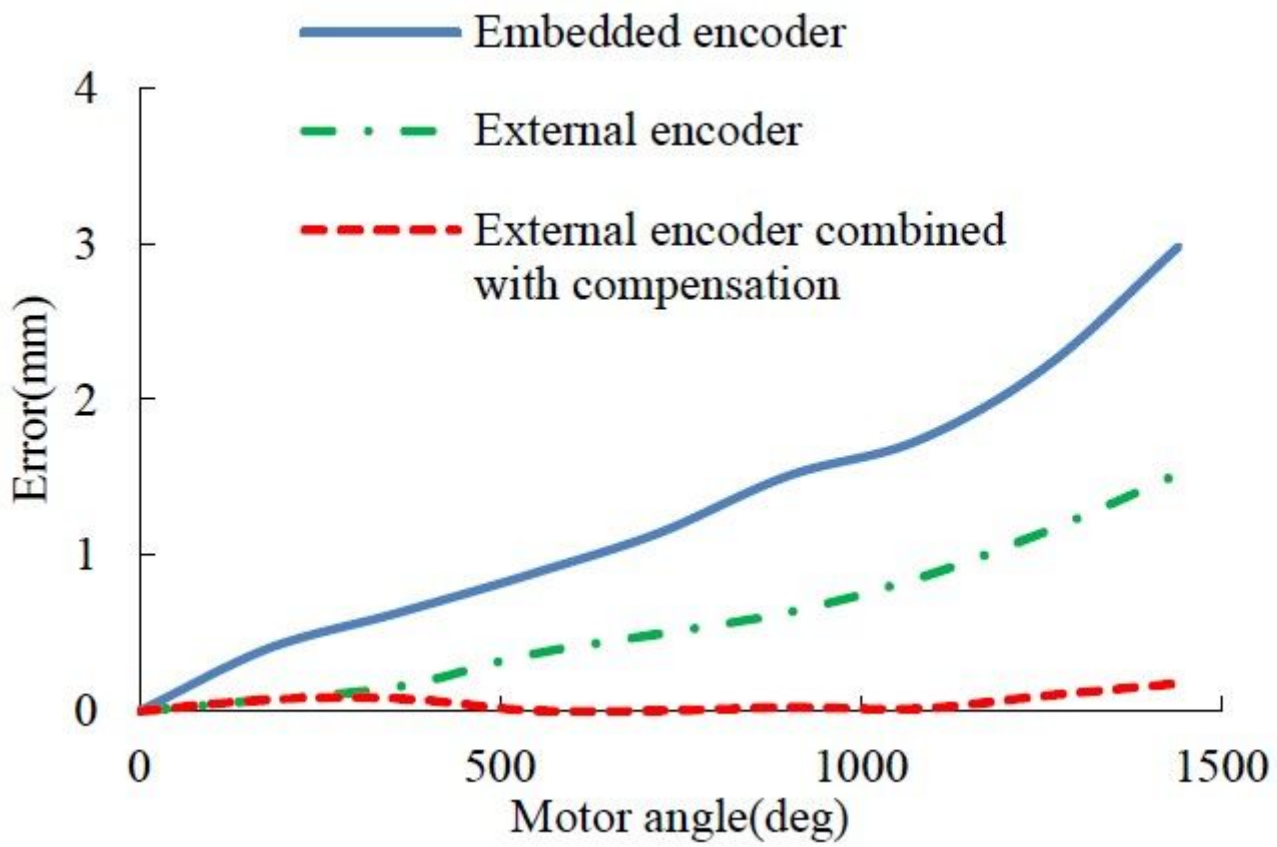

Figure 5

Comparison of the accumulated errors of the cable length measured by embedded motor encoder, external encoder and external encoder with compensation

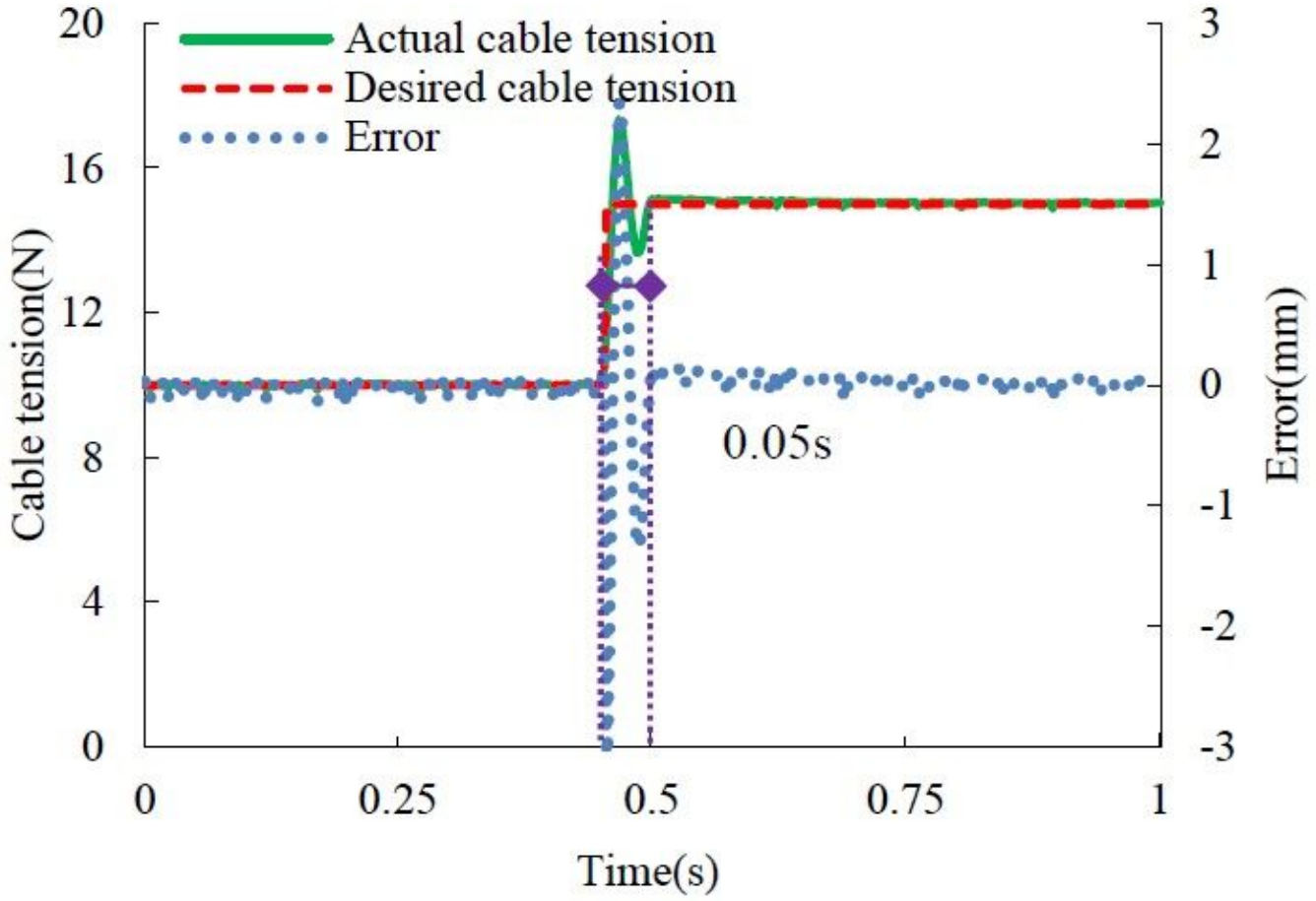

Figure 6

Response of the module with step signal input: actual cable tension, desired cable tension and their error

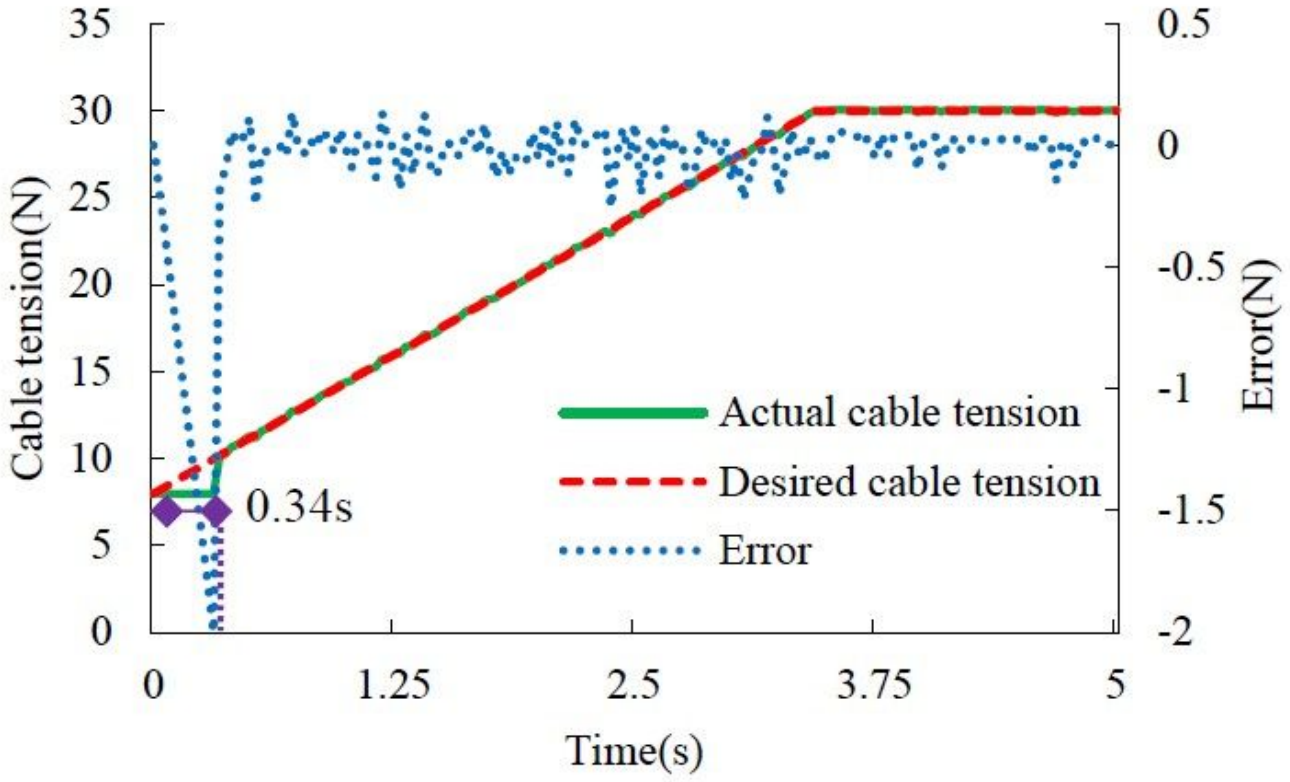

Figure 7

Response of the module with ramp signal input: actual cable tension, desired cable tension and their error

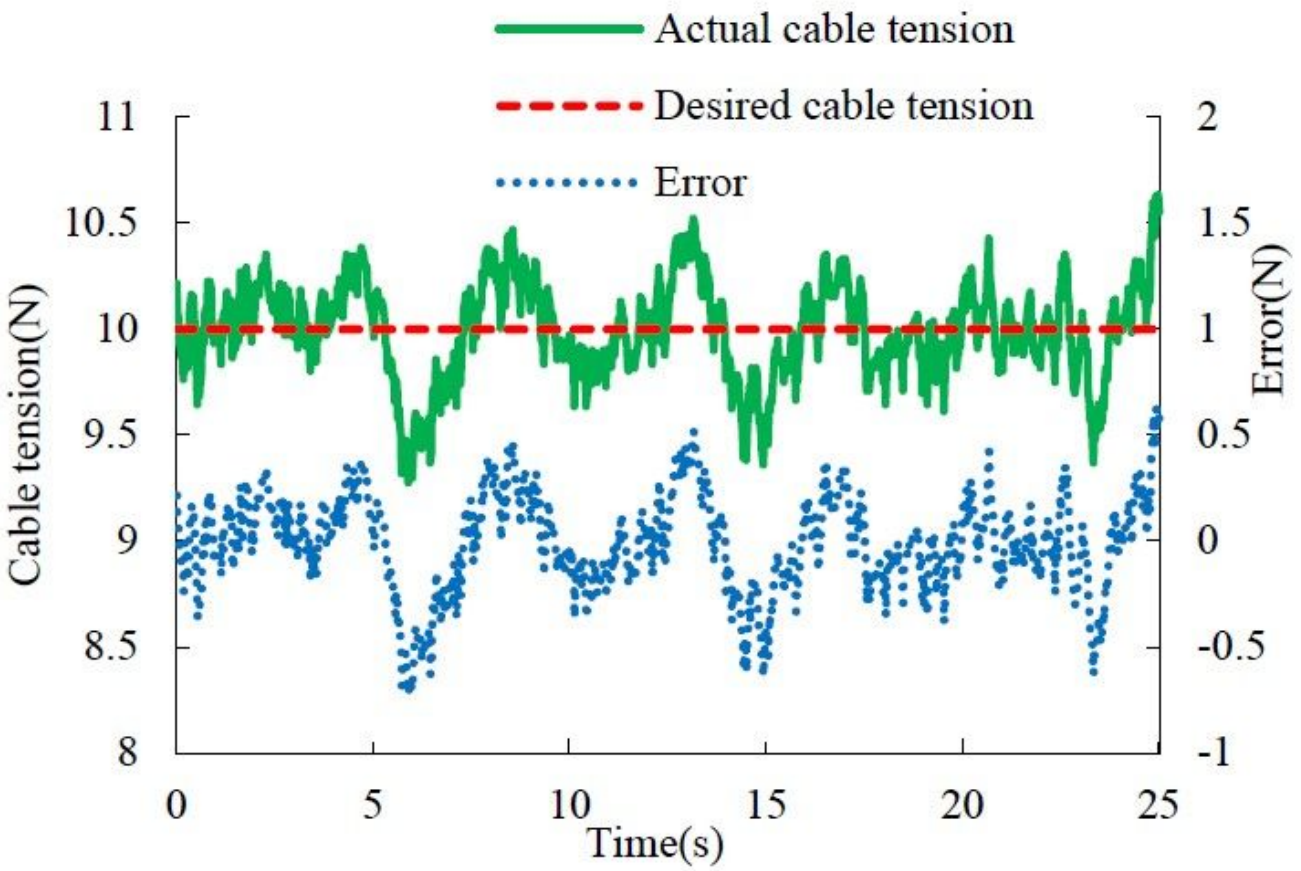

Figure 8

Variation of the actual cable tensions in reciprocating movement: actual cable tension, desired cable tension and their error

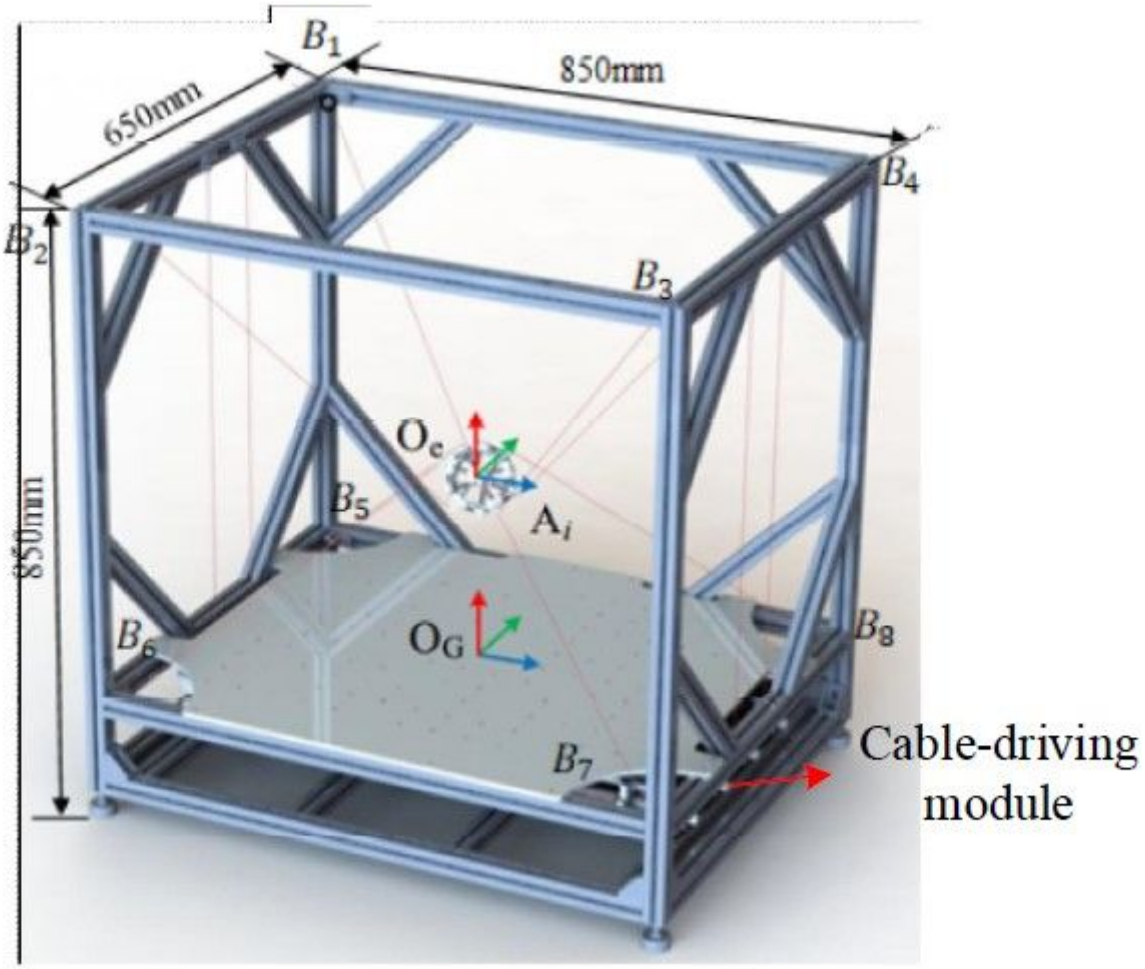

Figure 9

Structure of the 6-DOF CDPR driven by 8 cables

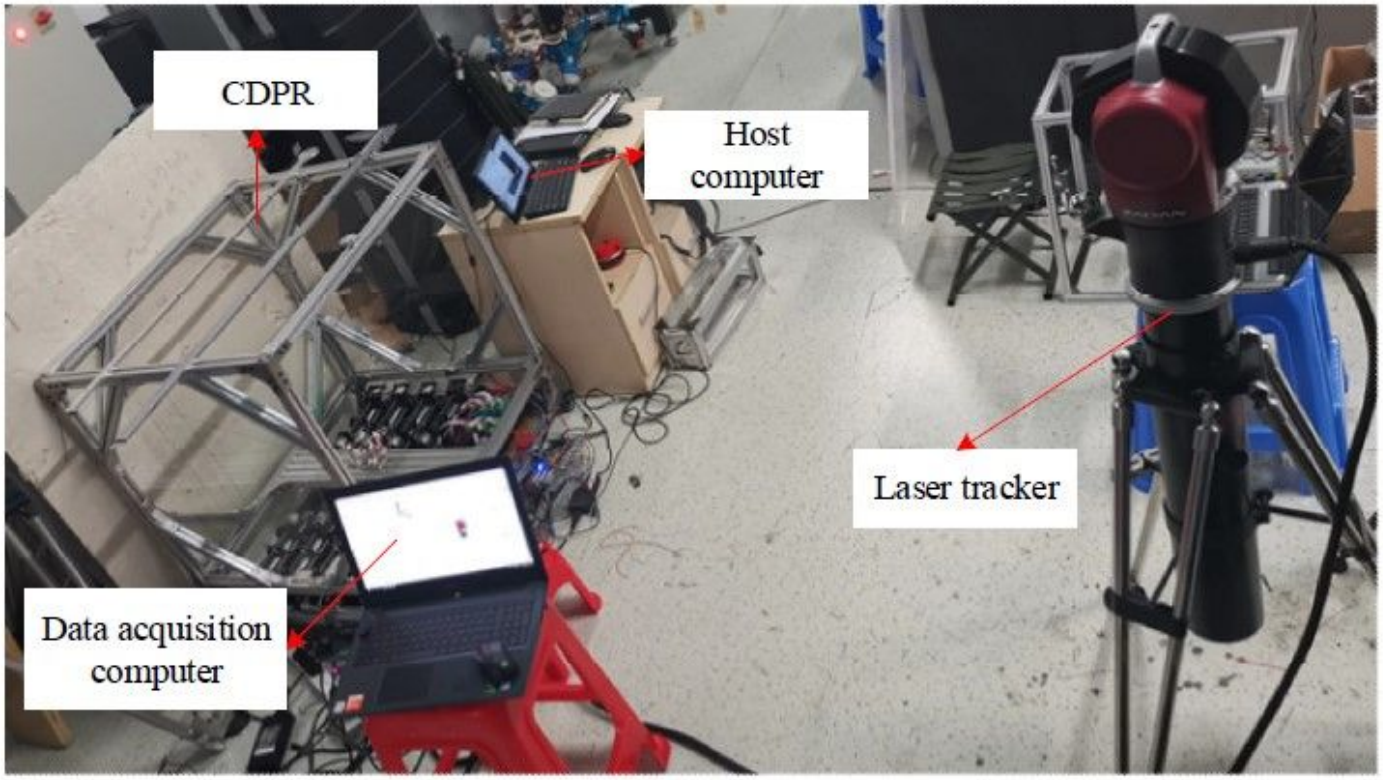

Figure 10

Experimental setup for the 6-DOF CDPR tests

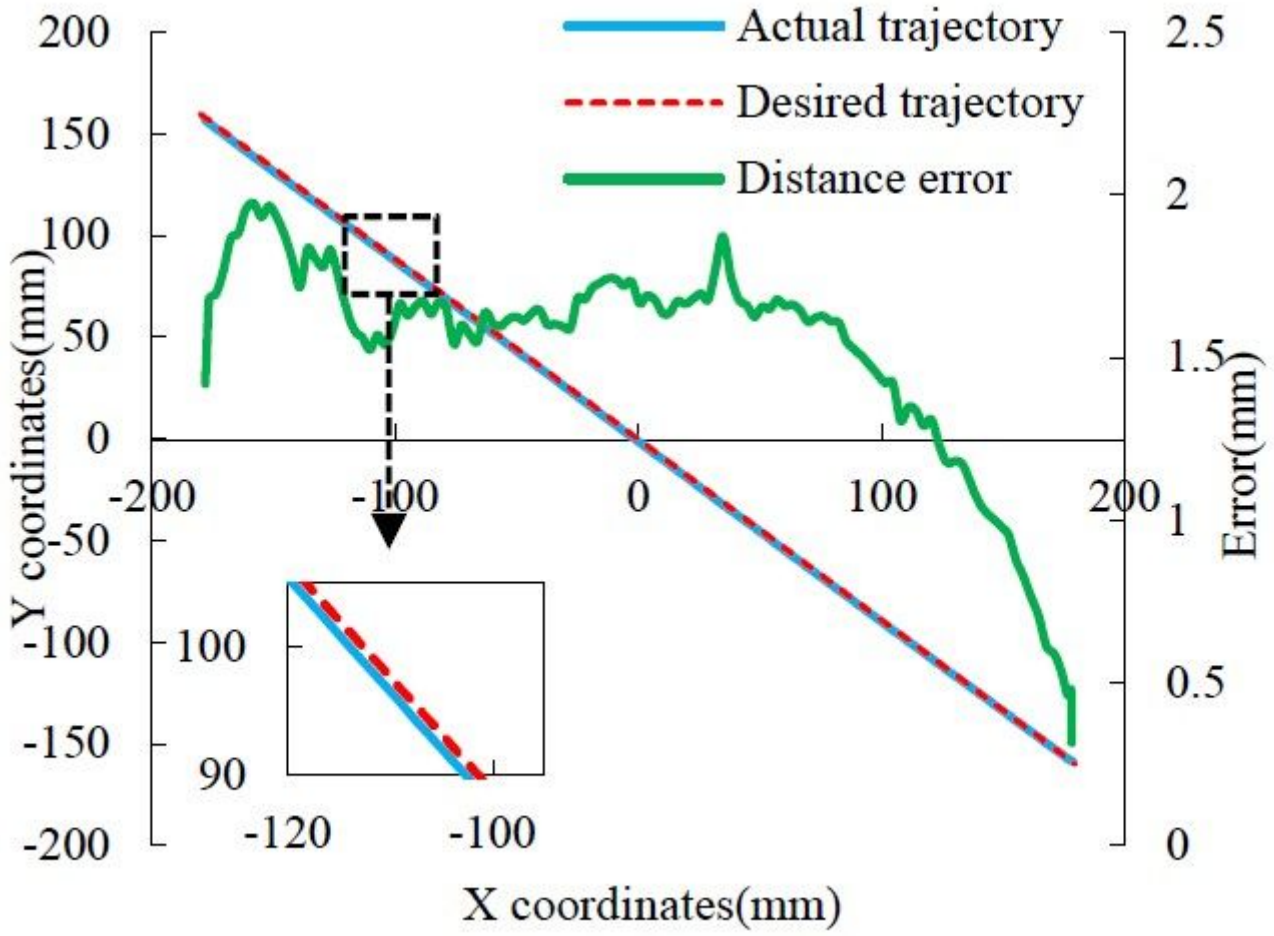

Figure 11

Line trajectory test: actual trajectory, desired trajectory and their error

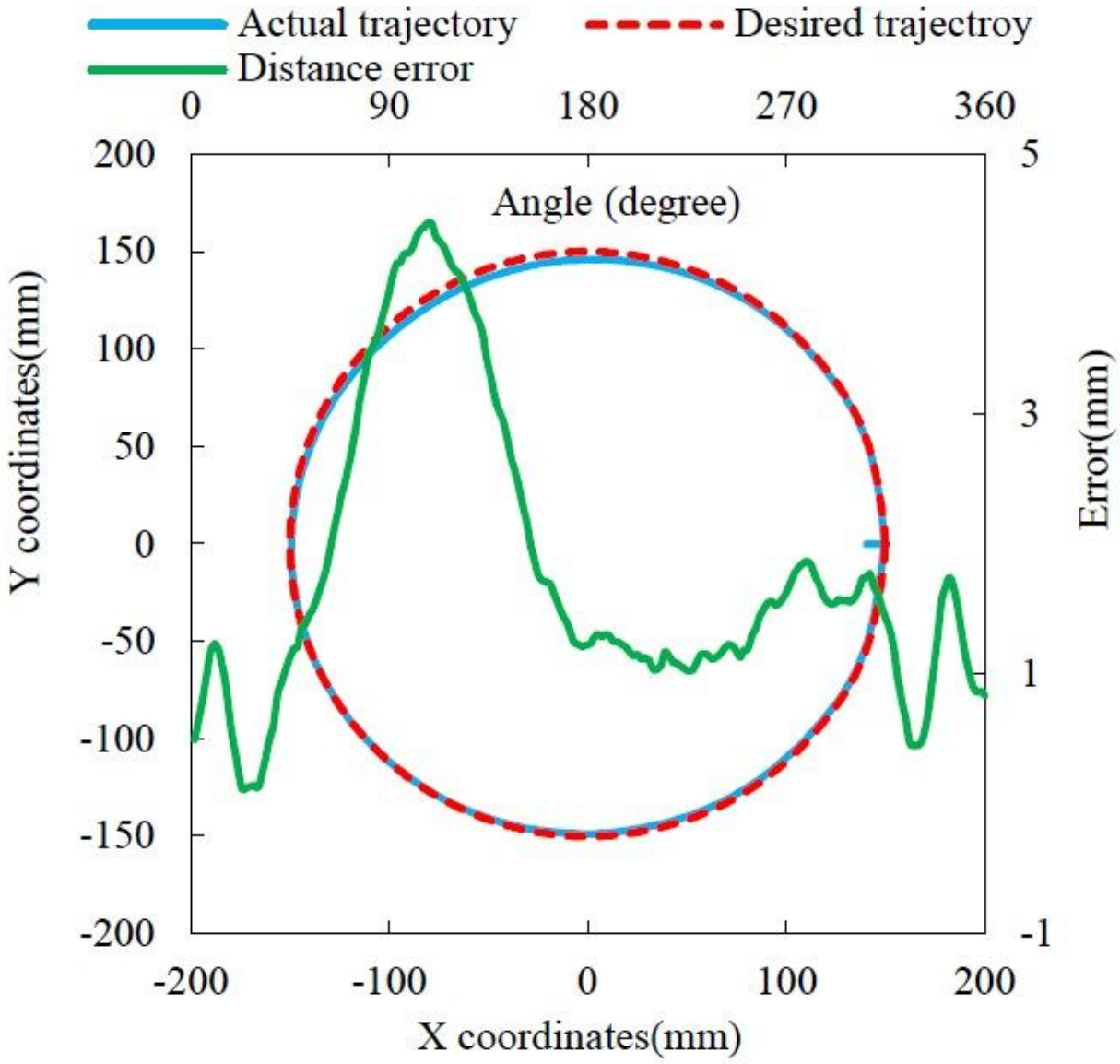

Figure 12

Circle trajectory test: actual trajectory, desired trajectory and their error

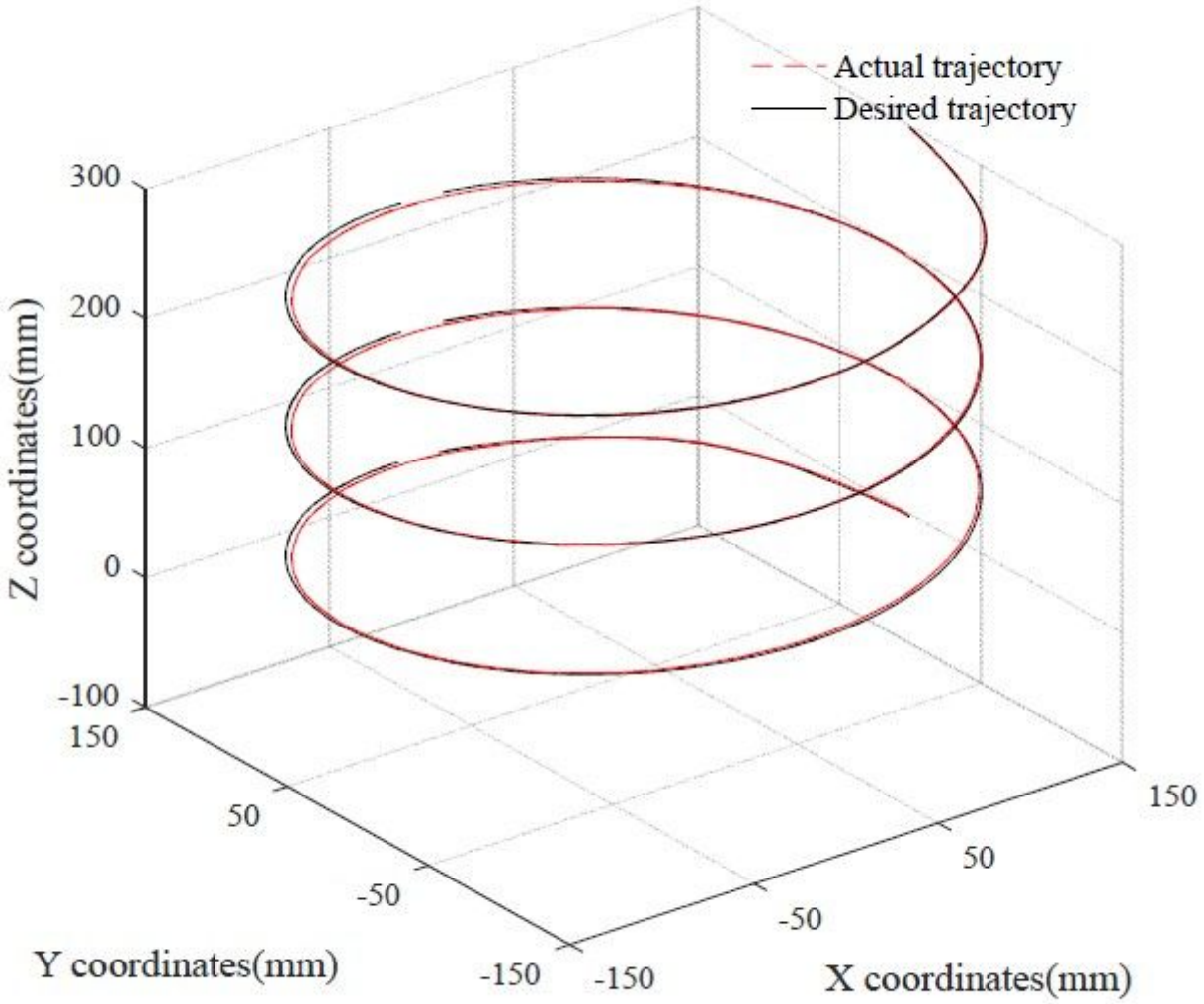

Figure 13

Space spiral trajectory test: actual trajectory and desired trajectory

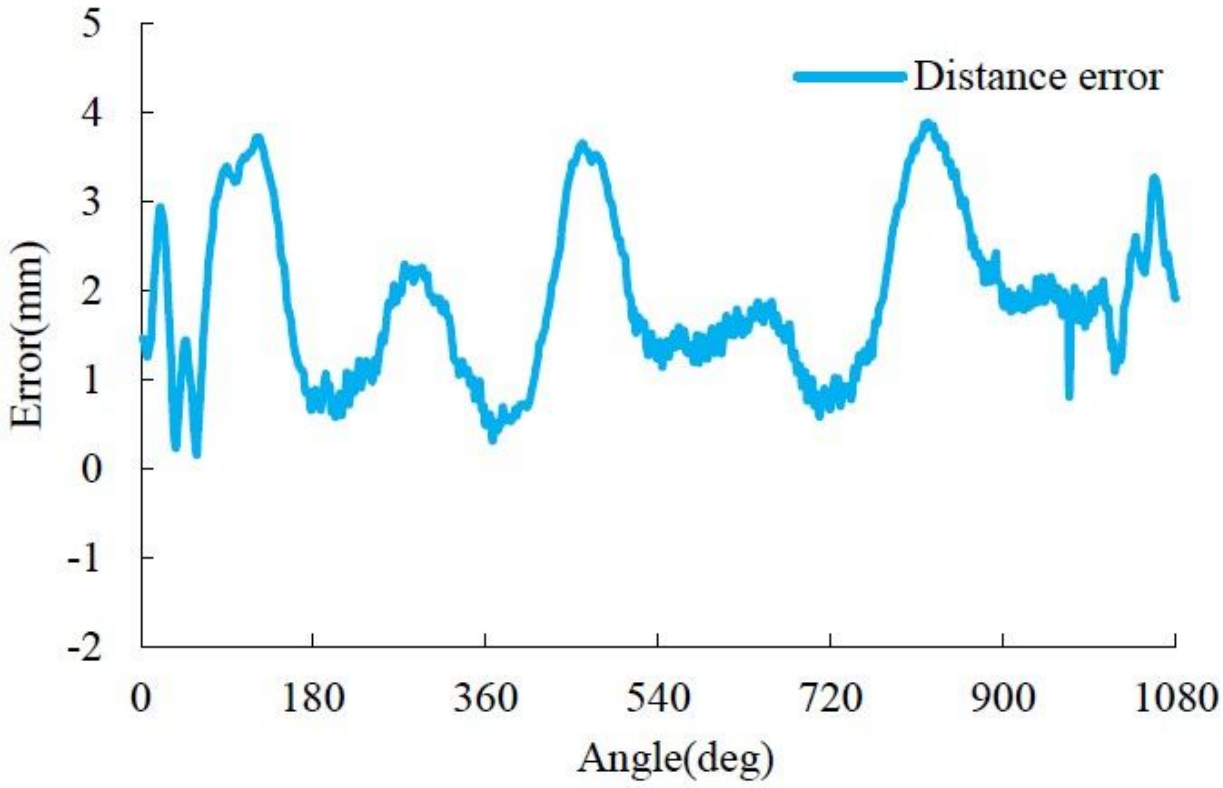

Figure 14

Error of the spiral trajectory test.

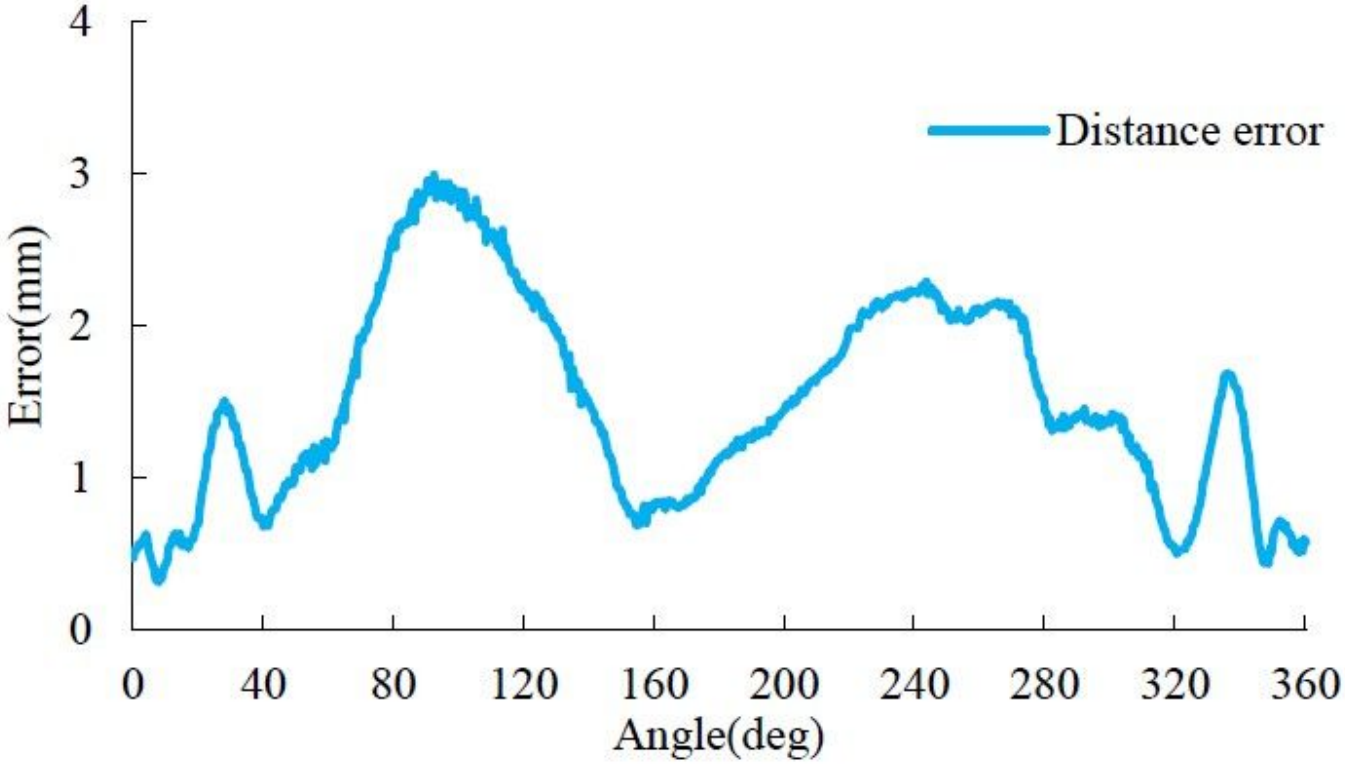

Figure 15

Errors of the circle trajectory between desired trajectory and actual trajectory under large load condition

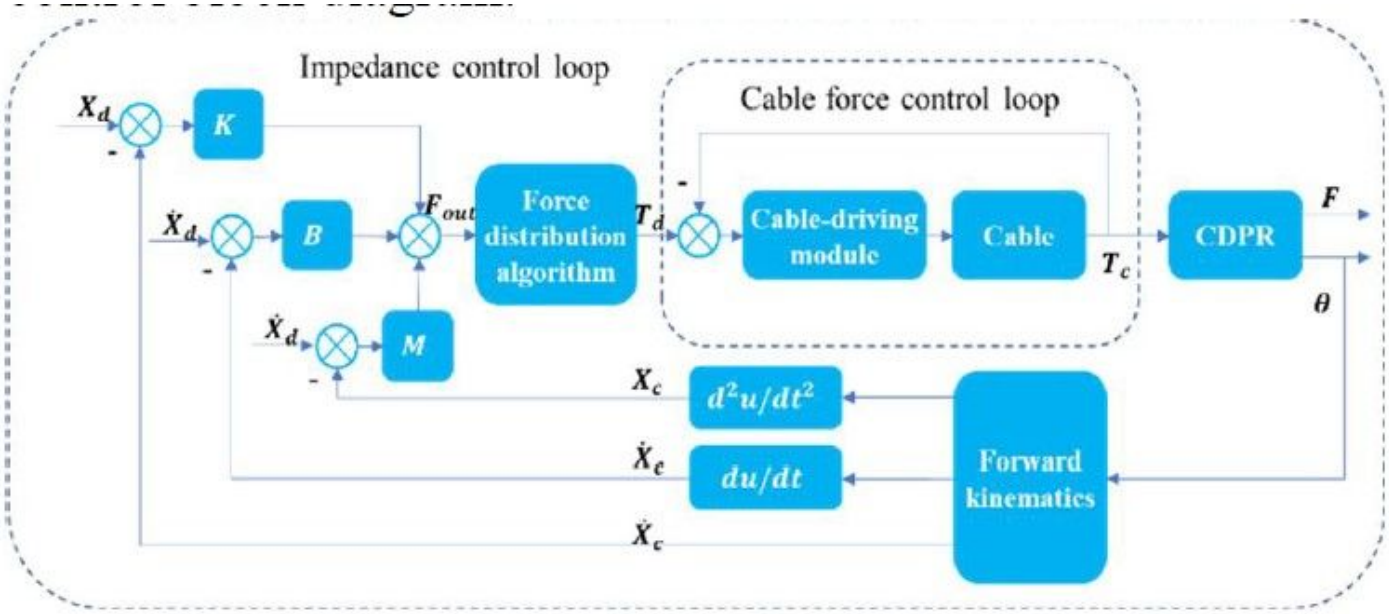

Figure 16

Control diagram of the impedance control mode

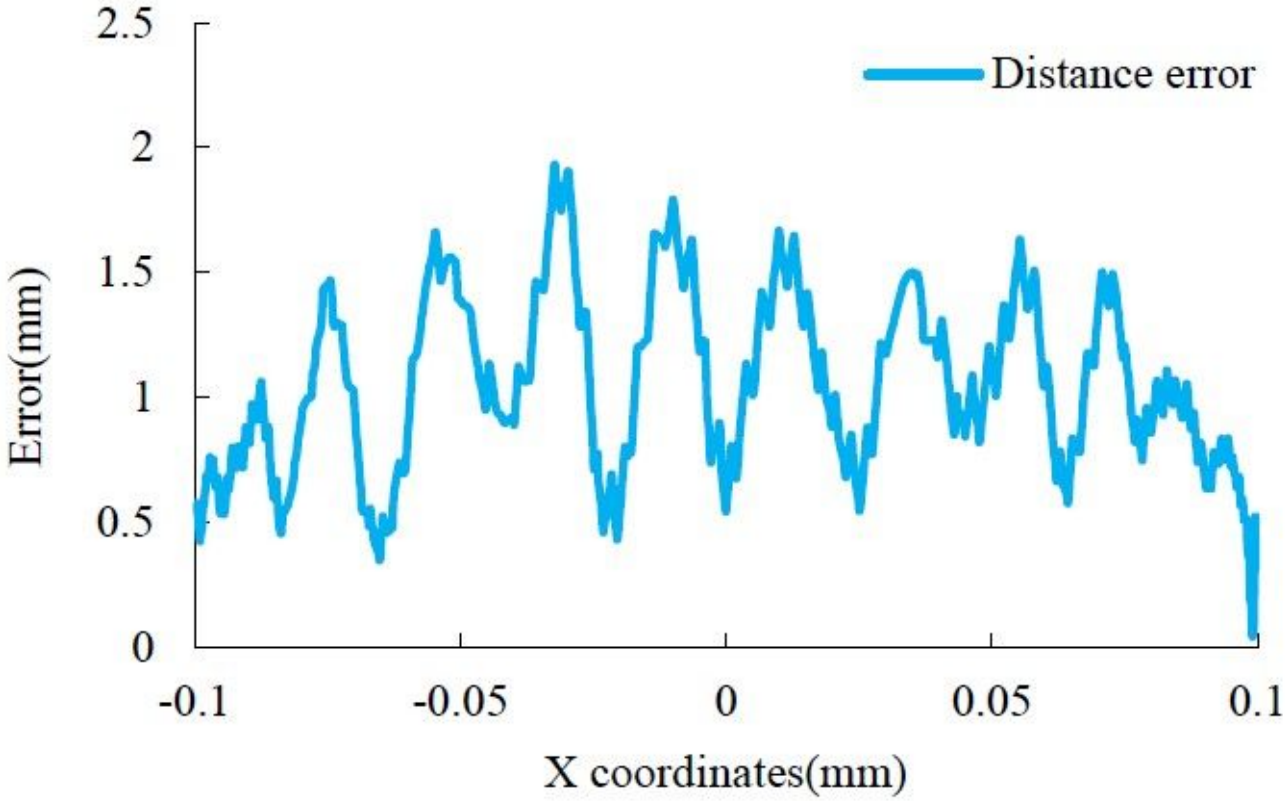

Figure 17

Trajectory tracking error between the actual and desired end-effector positions under impedance control mode

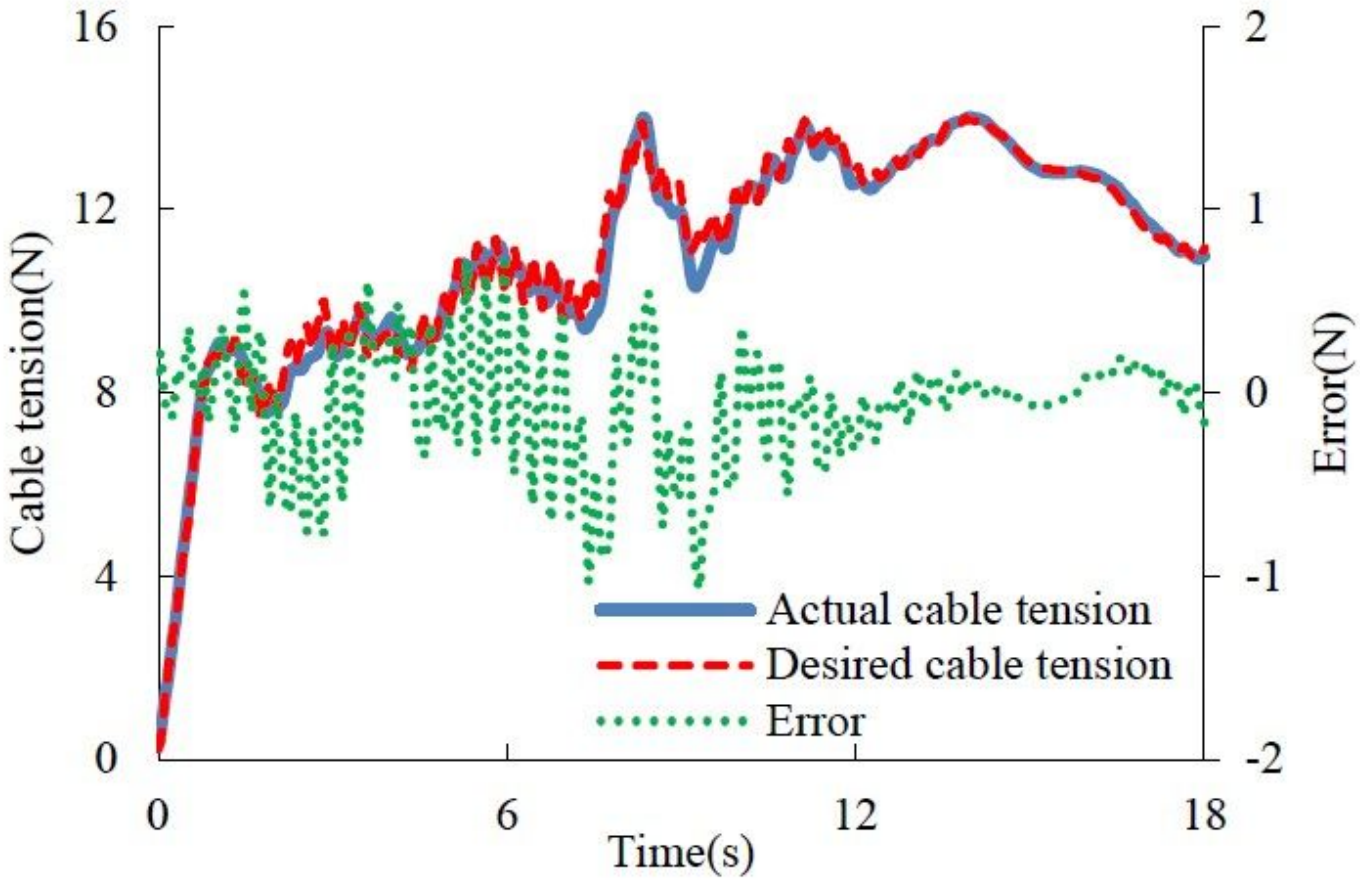

Figure 18

Variation of the cable tension in one of the 8 modules: desired cable tension, the actual cable tension and their error

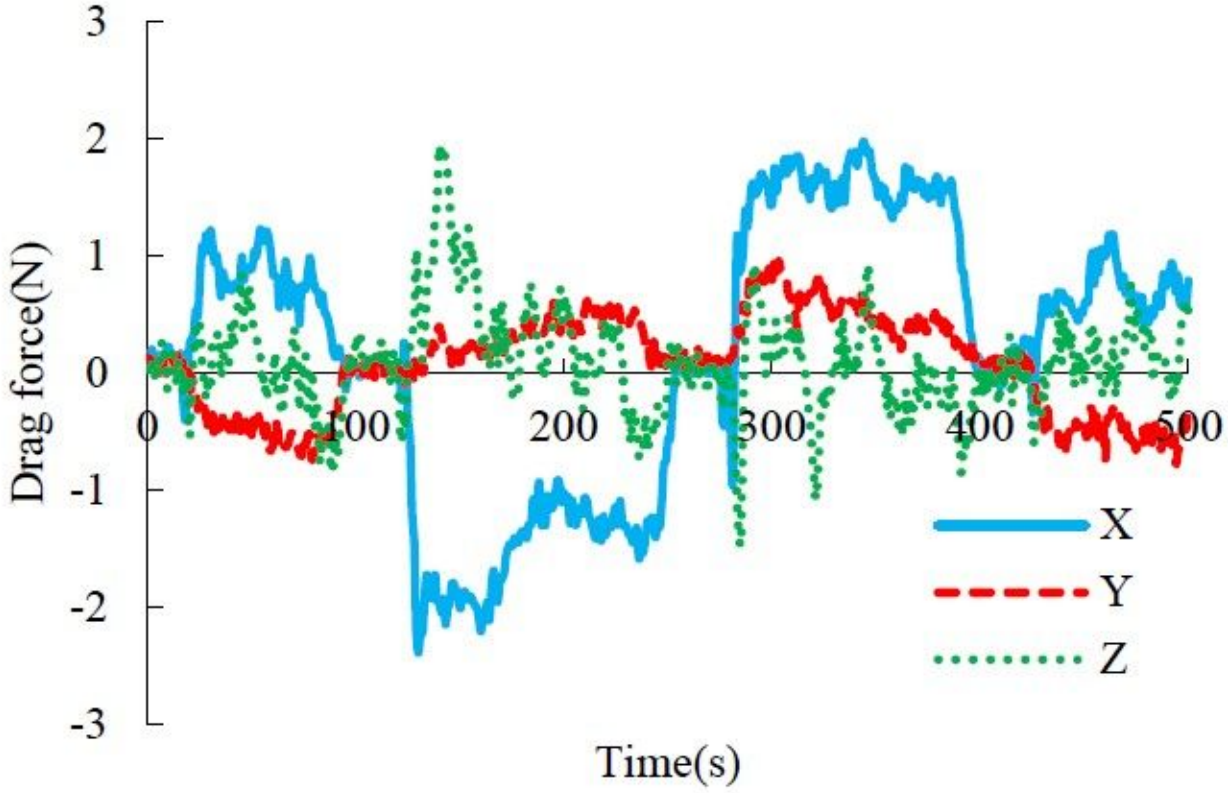

Figure 19

Variation of the drag force on the moving platform in three directions under direct teaching test